Biomedicine & Pharmacotherapy 142 (2021) 111948

Contents lists available at ScienceDirect

Biomedicine & Pharmacotherapy

journal homepage: www.elsevier.com/locate/biopha

Phenolics from *Physalis peruviana* fruits ameliorate streptozotocin-induced diabetes and diabetic nephropathy in rats via induction of autophagy and apoptosis regression

Shahira M. Ezzat [a,b], Heba M.I. Abdallah [c], Noha N. Yassen [d], Rasha A. Radwan [e], Eman S. Mostafa [b], Maha M. Salama [a,f,*], Mohamed A. Salem [g]

[a] Department of Pharmacognosy, Faculty of Pharmacy, Cairo University, Kasr El-Aini Street, Cairo 11562, Egypt
[b] Department of Pharmacognosy, Faculty of Pharmacy, October University for Modern Sciences and Arts (MSA), Giza 12451, Egypt
[c] Department of Pharmacology, Medical Research Division, National Research Centre (ID: 60014618), P.O. 12622, Dokki, Cairo, Egypt
[d] Department of Pathology, Medical Research Division, National Research Centre (ID: 60014618), P.O. 12622, Dokki, Cairo, Egypt
[e] Department of Biochemistry, Faculty of Pharmacy, Sinai University, East Kantara Branch, New City El Ismailia 41611, Egypt
[f] Department of Pharmacognosy, Faculty of Pharmacy, The British University in Egypt, El Sherouk City, Suez Desert Road, Cairo 11837, Egypt
[g] Department of Pharmacognosy, Faculty of Pharmacy, Menoufia University, Gamal Abd El Nasr st., Shibin Elkom 32511, Menoufia, Egypt

ARTICLE INFO

Keywords:
Diabetic nephropathy
Autophagy
Apoptosis
AMPK/mTOR pathway
Golden berry

ABSTRACT

The objective of our study was to evaluate the effect of *Physalis peruviana* L. fruits in the management of diabetes and diabetic nephropathy in relation to its metabolic profile. *In-vitro* α-amylase, β-glucosidase, and lipase inhibition activities were assessed for the ethanolic extract (EtOH) and its subfractions. Ethyl acetate (EtOAc) fraction showed the highest α-amylase, β-glucosidase, and lipase inhibition effect. *In vivo* antihyperglycemic testing of EtOAc in streptozotocin (STZ)-induced diabetic rats showed that it decreased the blood glucose level, prevented the reduction in body weight, improved serum indicators of kidney injury (urea, uric acid, creatinine), and function (albumin and total protein). EtOAc increased autophagic parameters (LC3B, AMPK) and depressed mTOR contents. Histopathology revealed that EtOAc ameliorated the pathological features and decreased the glycogen content induced by STZ. The immunohistochemical analysis showed that EtOAc reduced P53 expression as compared to the STZ-diabetic group. UPLC-ESI-MS/MS metabolite profiling of EtOAc allowed the identification of several phenolic compounds. Among the isolated compounds, gallic acid, its methylated dimer and the glycosides of quercetin had promising α-amylase and β-glucosidase inhibition activity. The results suggest that the phenolic-rich fraction has a protective effects against diabetic nephropathy presumably via enhancing autophagy (AMPK/mTOR pathway) and prevention of apoptosis (P53 suppression).

1. Introduction

Diabetes mellitus (DM) is a metabolic disorder that is featured by elevated blood sugar due to impaired insulin synthesis or decreased response to insulin. The high blood sugar leads to polydipsia, polyuria, and polyphagia [1]. DM is categorized as a chronic disorder with adverse effects on the metabolism of fats, proteins, and carbohydrates leading to serious acute or chronic complications [2]. Chronic hyperglycemia may affect the functions of kidneys, retina, and/or nerves leading to nephropathy, retinopathy, and/or neuropathy, respectively [3]. Disorders in glucose metabolism are one of the main causes of diabetes. Glucose is obtained from starch and other carbohydrates through their hydrolysis by α-amylase and glucosidases resulting in postprandial hyperglycemia [4]. High blood glucose levels cause glycosylation of nucleic acids, lipids, and proteins which is the main cause for the appearance of diabetic complications [5]. Prevention of after-meal absorption of carbohydrates can prevent the postprandial hyperglycemia. This can be achieved by inhibition of the pancreatic enzymes such as amylase and lipase together with the intestinal glucosidases. The inhibition of these digestive enzymes will reduce the release

* Correspondence to: Department of Pharmacognosy, Faculty of Pharmacy, Cairo University, Kasr El-Ainy St., Cairo 11562, Egypt.
E-mail addresses: shahira.ezzat@pharma.cu.edu.eg (S.M. Ezzat), hm.abdullah@nrc.sci.eg (H.M.I. Abdallah), nn.yassin@nrc.sci.eg (N.N. Yassen), rashaaradwan2011@gmail.com (R.A. Radwan), emostafa@msa.eun.eg (E.S. Mostafa), maha.salama@pharma.cu.edu.eg (M.M. Salama), mohamed.salem@phrm.menofia.edu.eg (M.A. Salem).

https://doi.org/10.1016/j.biopha.2021.111948
Received 3 April 2021; Received in revised form 10 July 2021; Accepted 14 July 2021
Available online 9 August 2021

of glucose and lipids and thus decrease their absorption and their elevated blood levels [6].

Diabetic neuropathy (DN) is a standout amongst the most complications of diabetes and it is described by hoisted level of serum creatinine, blood urea nitrogen, creatinine leeway, and also kidney hypertrophy [7]. Hyperglycemia could induce glomerulosclerosis, speeding the advance of DN. These progressions are an aftereffect of unusual glucose control, hemodynamic changes inside the kidney, and excessive oxidative stress [8]. Free radicals assault essential macromolecules prompting cell harm and homeostatic disturbance, obviously prompting the degenerative sicknesses that torment humanity [9]. DN is portrayed by a progression of renal structure variation from the norm including cellular layer thickening, mesangial extension, glomerulosclerosis, and tubule interstitial fibrosis [10].

Autophagy is a major catabolic pathway to maintain intracellular homeostasis leading to degradation, removing, and recycling of damaged or excess organelles and protein aggregates [11]. Studying autophagic mechanisms is rapidly advancing and showing that autophagy is involved in the pathogenesis of various diseases [11,12]. It has been noticed that autophagy has a protective role in several animal models including those for acute kidney injury [13–15]. The participation of autophagy in the pathogenesis of DN is arising. Autophagy can be induced by intracellular stresses such as nutrient-depleted conditions. The pathways of autophagy involve the mammalian target of rapamycin (mTOR), oxidized NAD (NAD^+) dependent histone deacetylase (Sirt1), and AMP-activated protein kinase (AMPK). Alteration of these pathways interferes with the autophagic stress responses, leading to aggravation of kidney dysfunction and the development of diabetic nephropathy [16].

One of the most successful ways to assess new drugs for controlling DM is trialing their effect on animals [17]. Administration of sterptozotocin (STZ) is a reliable method for the induction of diabetes in rats [18]. STZ is a broad-spectrum antibiotic that is toxic to the β-pancreatic cells which produce insulin [19]. Studies have been implemented to test the mechanism of action of STZ on the pancreatic cells, it was reported that STZ is taken by the cell membrane GLUT2 and alkylate DNA which leads to the eventual death of pancreatic β-cells [20,21]. Moreover, STZ's actions on protein alkylation and nitric oxide add to its cytotoxicity [22], as STZ enters through GLU2, its action is not specific to β-cells and can damage other tissues such as the kidney and liver [23]. STZ is commonly administered via two routes, intravenous and intra-peritoneal [24].

In the latest years, much attention has been focused on the biologically active compounds that are of natural resources. Many plants have bioactive metabolites for the management of diabetes and associated complications [25]. *Physalis peruviana* L. is a tropical plant belonging to the family Solanaceae, known in English as Golden berry and Cape gooseberry [26]. It is native to South America and grown in Egypt, India and New Zealand [27]. *P. peruviana* fruits have many active constituents such as vitamin A, E, B, C, E and K as well as minerals, polyunsaturated fatty acids, and carbohydrates [28]. Furthermore, hydroxyester disaccharides [29], withanolides (steroidal lactones) [30,31], as well as carotenoids [32] were also reported in the fruits. In addition, the fruits contain phenolic acids such as caffeic, gallic, chlorogenic, ferulic, and *p*-coumaric acids as well as flavonoids such as quercetin, rutin, myricetin, kaempferol, catechin, and epicatechin [33].

Golden berry fruits have long been used in folk medicine for the treatment of diabetes, hepatitis, malaria, dermatitis, asthma, and rheumatism [34]. Recent researches have reported that *P. peruviana* fruit powder or its methanolic extract in combination with chromium had antidiabetic and antioxidant activities in rats [35]. Also, the ethanolic extract of the fruits improved insulin sensitivity and ameliorated hyperglycemia in high-fat diet-induced type 2 diabetic rats [36]. Moreover, the ethanolic extract of the fruits showed a protective effect against acute renal damage in rats [33]. However, the mechanisms of the antidiabetic activity of *P. peruviana* fruits in relation to its chemical profile have not been deeply elucidated. Accordingly, we aimed to evaluate the antidiabetic as well as the curative effects of golden berry fruits against diabetic complications through a bio-guided fractionation protocol. In addition to the isolation of its major metabolites and evaluating their antidiabetic action. The α-amylase, β-glucosidase, and lipase inhibition activities of the ethanolic extract of the fresh fruits along with its different sub-fractions, were assesses to select the active fraction. The active fraction was tested in vivo for its antidiabetic activities and studying underlying mechanisms in STZ-induced diabetic nephropathy in rats. Meanwhile, the chemical constituents of the active fraction were studied using ultra-high-performance liquid chromatography coupled to electrospray ionization- tandem mass spectrometry (UPLC-ESI-MS/MS) analysis with the isolation of the major detected metabolites, which were also evaluated for their in vitro α-amylase, β-glucosidase and lipase inhibition activities.

2. Material and methods

2.1. General

β-NADPH, potato starch, 3,5-dinitrosalicylic acid, β-glucosidase enzyme, *p*-nitro phenyl-β-D-glucopyranoside (PNGP), bovine serum albumin (BSA), 1-deoxynojrimycin, DMSO, streptozotocin, quercetin, pancreatic lipase, 4-nitrophenyl octanoate (NPC), sodium acetate, Tris-HCl and analytical solvents were purchased from Sigma-Aldrich (St, Louis, MO). Acarbose was purchased from Bayer Pharmaceuticals Pty, Ltd. (Wayne, NJ). Orlistat and Gliclazide were obtained from Servier Canada (Laval, QC, Canada). Diagnostic kits for measuring glucose, creatinine, urea, uric acid, albumin, and total protein were obtained from Biodiagnostic, Egypt. LC3II, AMPK, and mTOR were determined using enzyme-specific immunosorbent assay kits obtained from Glory Science (Del Rio, Texas, USA). P53 staining was done using a kit provided by Abcam, UK. High-resolution ESI mass spectra were measured using an orbitrap-type FT mass spectrometer (Thermo Fisher Scientific, Bremen, Germany). UV recordings were made on a Shimadzu UV–Visible-1601 spectrophotometer. NMR spectra were acquired in DMSO-d6 in a Brucker 400 MHz NMR spectrometer, at 400 MHz. Standard pulse sequence and parameters were used to obtain one-dimensional 1 H and ^{13}C spectra. ^{1}H chemical shifts (δ) were measured in ppm, relative to TMS, and ^{13}C NMR chemical shifts to DMSO-d6 and were converted to TMS scale by adding 39.5. Paper chromatographic analysis (PC) was carried out on Whatman No. 1 paper, using solvent systems: (1) H_2O; (2) 2% HOAc (acetic acid: H_2O, 98:2); (3) BAW (n-BuOH–HOAc-H2O, 4:1:5, upper layer); (4) B BPW (Benzene-n-BuOH–Pyridine– H2O, 1:5:3:3, upper layer).

2.2. Plant material

The Agricultural Research Center, Giza, Egypt supplied the authors with the fruits of *P. peruviana*. Authentication was approved by Prof. Dr. Wafaa Amer, Department of Botany, Faculty of Science, Cairo University, Giza, Egypt. A voucher specimen (5–7–2015) was deposited at the herbarium of the Pharmacognosy Department, Faculty of Pharmacy, Cairo University, Cairo, Egypt.

2.3. Preparation of extracts and fractions

The fresh fruits (2 kg) were homogenized with 70% EtOH (5 L) overnight, then the solvent was filtered. The extraction was repeated three times and the combined ethanol extract was dried at 40 °C under vacuum to yield dark brown amorphous residue (220 g). The ethanolic residue (100 g) was suspended in distilled water (400 ml) and fractionated by liquid-liquid partitioning with methylene chloride (200 ml x 3 times), ethyl acetate (200 ml x 3 times), and *n*-butanol saturated with water (200 × 3 times). The solvent was, in each case, evaporated under vacuum to obtain 20, 40, and 10 g of MeCl, EtOAc, and BuOH fractions, respectively.

2.4. In vitro assays

2.4.1. α-Amylase inhibition assay

Potato starch was dissolved in 20 mmol/L sodium phosphate buffer with 6.7 mmol/L NaCl at pH 6.9. To prepare the enzyme solution: 25.3 mg of α-amylase (10 U/ml) was added to 100 ml of cold distilled water with stirring. The final concentration of the extracts under investigation-dissolved in a buffer- ranged from 1000 to 31.25 μg/ml. Sodium potassium tartrate solution (12.0 g of sodium potassium tartrate tetrahydrate in 8.0 ml of 2 M NaOH) was mixed with 96 mmol/L 3,5-dinitrosalicylic acid solution for the preparation of the colorimetric reagent. Then, control and extract were mixed with starch solution and set to react with α-amylase solution in alkaline medium at 25 ºC. The formation of maltose was deduced by the reduction of 3,5-dinitrosalicylic acid to 3-amino5-nitrosalicylicacid. The positive control used was acarbose. The reaction was detectable at 540 nm. Percentage of inhibition was calculated by using the following formula: 100- [(A_{sample}/ $A_{control}$) x 100] [37].

2.4.2. β-Glucosidase inhibition assay

0.1 M sodium acetate buffer (0.1 ml), pH 5.0 and 0.5 ml of 20 mM *p*-nitrophenyl β-D-glucopyranoside (PNPG) solution were mixed and equilibrated at 37 ºC for about 5 min, before adding 0.5 ml of the enzyme solution (β-glucosidase) dissolved in ice-cold 50 mM Tris-HCl buffer pH 7.8, diluted in 10 mM phosphate buffer, pH 7.0 containing 0.2% of BSA to 0.006–0.022 U/ml. After 15 min incubation at 37 °C, 2.0 ml of Na_2CO_3 solution was added to stop the reaction and the optical density was measured at 400 nm. The blank was prepared by mixing the reaction mixture with 2.0 ml of Na_2CO_3 solution after 15 min-incubation at 37 °C, followed by the addition of the enzyme solution. Percentage of inhibition was calculated by using the following formula: % Inhibition = 100-[(A_{sample}/ $A_{control}$) x 100] [38].

2.4.3. Pancreatic lipase inhibition

The method was applied adopting Conforti and colleagues [39]: An aqueous solution (1 mg/ml) type II crude porcine pancreatic lipase was prepared. In addition,5 mmol/L solution of 4-nitrophenyl octanoate (NPC) in DMSO. The reaction mixture was: 100 μl of 5 mmol/L NPC+ 4 ml of Tris-HCl buffer (pH =8.5) + 100 μl of extract + 100 μl of enzyme solution. The mixture was incubated at 37 °C for 25 min prior to the substrate addition. The control used 100 μl DMSO, a blank sample-without the enzyme- was measured for each extract. The absorbance was determined at 412 nm. Orlistat at a final concentration of 20 μgm/L was tested for comparison. Percentage of inhibition was calculated by using the following formula: %Inhibition = 100-[(A_{sample}/$A_{control}$) x 100].

2.4.4. Determination of radical scavenging activity (DPPH assay)

The assay is based on reducing DPPH (2,2-diphenyl-1-pycrylhydrazyl), a stable radical, with an antioxidant and measuring the absorbance at 517 nm [40]. The reaction mixture was as follows: 500 μl of the tested extracts or isolates+ 375 μl ethanol + 125 μl of a 1 mM freshly prepared DPPH solution in ethanol. Different concentrations of the test samples were prepared while the final concentration of DPPH in the reaction mixture was 0.125 mM. After incubation of the mixture at 37 °C for 30 min in the dark, the absorbance was measured at 517 nm. Blank samples contained the same amount of ethanol and DPPH solution. All experiments were carried out in triplicate. Ascorbic acid was used as a positive control. Percentage radical scavenging activity of samples was calculated using the radical scavenging activity: (%) = (A_{blank} – A_{sample}/ A_{blank}) x 100.

2.4.5. Oxygen radical absorbance capacity (ORAC assay)

Tested samples were dissolved in phosphate-buffered saline (10 mM, pH 7.4) and investigated for their antioxidant capacity. The antioxidant capacity was measured by determining the time course of the fluorescence decay of fluorescein, induced by 2,2′-azobis (2-amidinopropane) dihydrochloride (AAPH) compared with Trolox, (6-hydroxy-2,5,7,8-tetra-methylchroman-2-carboxylic acid, used as a positive control [41, 42].

2.4.6. Statistics

The IC_{50} (concentration necessary for 50% inhibition of enzyme activity) was calculated by constructing a linear regression curve showing extracts concentrations (from 75 to 600 μg/ml) for α-amylase, (from 60 to 600 μg / ml) for β -glucosidase and from (75–120 μg/ml) for pancreatic lipase on the x-axis and percentage inhibition on the y-axis [43]. All analysis was done using the SPSS v. 22.0 (IBM, Chicago, USA). Microsoft Excel 2010 was used for graphs construction.

2.5. In vivo evaluation of the antidiabetic activity

2.5.1. Induction of diabetes

Adult male albino rats (Wistar strain, 200 – 250 g; age, 28–30 weeks) and male mature albino mice of 20 – 25 g and age, 5–7 weeks were obtained from the animal house colony of the National Research Center, Egypt. All experimental procedures were conducted following internationally accepted principles for laboratory animal use and care and were approved by the Ethics Committee, Faculty of Pharmacy Cairo University, Cairo, Egypt (Approval no: MP 2164). Acute toxicity studies were performed on the mice. Different doses of EtOAc fraction up to 2000 mg/kg were given. Then, the animals were observed for 24 h for mortality [44].

Diabetes was induced in the rats by a single i.p. dose of STZ (55 mg/kg) [45]. Rats with serum glucose levels above 250 mg/dl were chosen and considered diabetic. EtOAc fraction was tested in the diabetic rats at two dose levels (50 and 100 mg/kg) for two weeks (based on the results of acute toxicity study). A group of normal rats was kept as a negative control, while, another group of diabetic rats receiving no treatment was considered as a positive control. An animal group receiving the standard antidiabetic gliclazide was also considered. In all cases, each group consisted of six rats. After the two weeks, the rats were kept for overnight fasting and the blood samples were collected and left at room temperature for 30 min. The samples were centrifuged for 20 min at 5000 rpm then the serum was separated and stored at − 80 °C for the analysis. The samples were analyzed for serum glucose, creatinine, urea, uric acid, albumin, and total protein using the corresponding diagnostic kits based on the instructions of the company.

2.5.2. Determination of autophagy-related parameters

Aliquots of the pancreas and kidney of the sacrificed animals were instantaneously dissected and homogenized in 20% (w/v) ice-cold phosphate buffer. The homogenate was then centrifuged via a cooling centrifuge at 1538 g for 5 min and the obtained supernatant was used for determining pancreatic and renal contents of LC3II, AMPK, and mTOR using enzyme-specific immunosorbent assay kits per the producer's instructions (MyBioSource, Inc., San Diego, USA).

2.5.3. Histopathology

Aliquots of pancreatic, kidney, and liver tissues of all animals were cut into specimens. Then fixed in 10% neutral-buffered formalin saline for 72 h. All the specimens were rinsed in tap water for 30 min and then dried in ascending ratios of alcohol, cleared in xylene, and fixed in paraffin. Serial sections of 5 μm thick were cut and stained with haematoxylin and eosin for histopathological investigation or stained by Periodic Acid Schiff (PAS) for glycogen detection.

2.5.4. Immunohistochemistry for detection of P53 expression

Paraffin-embedded blocks were sectioned at 5 μm thickness. The sections were deparaffinized and rehydrated via a descending series of alcohol then distilled water, incubated with sodium citrate buffer in a humidity-heat chamber to retrieve antigen. As for endogenous peroxidase deactivation, this was achieved by hydrogen peroxide also the non-

specific bindings were blocked with a protein-blocking reagent. The prepared sections were further incubated with rabbit polyclonal anti-P53 antibody, then with horseradish peroxidase conjugate, and then with complement solution. Finally, the reactions were revealed with 3–3'diaminobenzidine and the sections were stained with hematoxylin as a contrast. Examination of slides was performed by the high magnification power to semi-quantitatively identify focally and completely stained cells which are defined as positive for the markers.

2.5.5. Immuno-histomorphometric quantitation

Additional histopathological evaluation was achieved via a quantitative morphometric analysis of the pathological alteration. The area of the tissue showing damaged cells with included nuclei, which were intensely stained, using P53 immunohistochemical expression as well as detection of area % of glycogen content using PAS histochemical stain was detected by a computer-assisted automated image analyzer. A Leica QWin image processing and analysis system (Cambridge, UK, Image Analyzer Unit; Pathology Department, National Research Center, Cairo, Egypt) was used for interactive automatic measurement of the percentage of damaged areas on slides stained with hematoxylin and eosin through examining ten random fields per slide.

2.6. UPLC-ESI-MS/MS analysis

The metabolites of EtOAc were separated on RP High Strength Silica (HSS) T3 C18 column (100 mm × 2.1 mm containing 1.7 μm diameter particles, Waters), using a Waters Acquity UPLC system. The mass spectra were acquired by full scan MS in positive and negative ionization mode on an Exactive high-resolution Orbitrap-type MS (Thermo Fisher, Bremen, Germany)[46].

2.7. Isolation of the major compounds

On a Sephadex LH-20 (850 g) column (100 × 7.5 cm, EtOAc fraction (15 g) was applied and eluted with H_2O then H_2O/EtOH mixtures in decreasing ratio, where, eight fractions (I–VIII) were separately obtained, dried in vacuum and subjected to 2D-PC. Compound **1** (35 mg) was isolated from fraction II (1.13 g, eluted with 10% aq. MeOH), by purification over 10 g Sephadex LH-20 column using MeOH / H_2O mixture for elution. Compound **2** (30 mg) was isolated from fraction III (850 mg, eluted with 20% aqueous methanol), by fractionation on a Sephadex LH-20 (15 g) column using 40% aqueous MeOH for elution. Compounds, **3** (20 mg), **4** (33 mg) and **5** (45 mg) were individually isolated from fraction IV (900 mg, eluted with 30% aqueous methanol) by Preparative PC, using *n*-BuOH saturated with water as a solvent. Fraction V (658 mg, eluted with 40% aqueous methanol) was applied on a polyamide column (50 g) and gradient elution with water/MeOH mixture of decreasing polarities, where, two successive subfractions were obtained; subfractions i and ii, at 20% and 30% aq. MeOH, respectively. Purification of subfraction i and ii by preparative PC using BAW as a solvent system afforded Compounds **6** (26 mg) and **7** (36 mg).

Fraction VIII (590 mg, eluted with 90%) was fractionated over a polyamide-s6, using a solvent mixture of MeOH: Benzene: H_2O (60:38:2) for elution, the individually collected subfractions were separately purified by crystallization from EtOH, thus yielding pure samples of compounds, **8** (33 mg), **9** (19 mg) and **10** (46 mg).

Compound 1 (35 mg) was obtained as a non-crystalline amorphous white powder, with negative ESI-MS: $[M-H]^-$: 483.08691 calculated for $C_{20}H_{20}O_{14}$. **Compound 2** (30 mg) was obtained as yellowish-white amorphous powder with negative ESI-MS, $[M-H]^-$ at *m/z* of 447.10817 corresponding to the molecular formula $C_{21}H_{20}O_{11}$. **Compound 3** (20 mg) was obtained as a yellowish white amorphous powder with a negative ESI-MS, [M-H]- at *m/z* of 463.98956, corresponding to the molecular formula $C_{21}H_{20}O_{12}$. **Compound 4** (33 mg) was obtained as off-white amorphous powder; $[M-H]^-$ molecular ion in its negative ESI/MS spectrum, at 169.02152, corresponding $C_7H_6O_5$. **Compound 5** (45 mg) was obtained as off-white amorphous powder with negative ESI-MS molecular ion peak $[M-H]^-$ at 483.08691 corresponding to to the molecular formula $C_{20}H_{20}O_{14}$, identical with those reported for digalloyl glucoses. **Compound 6** (26 mg) was obtained as yellow powder. It showed a negative ESI-MS $[M-H]^-$ at $m/z = 301.0354$ calculated for the molecular formula $C_{15}H_{10}O_7$. **Compound 7** (36 mg) was obtained as a yellow amorphous powder. It has a negative ESI-MS analysis ($[M-H]^-$ at $m/z = 285.0406$ with a molecular formula $C_{15}H_{10}O_6$. **Compound 8** (33 mg) was separated as yellow amorphous powder, it has a negative ESI-MS analysis ($[M-H]^-$ at *m/z of* 447.00123 calculated for the formula $C_{21}H_{20}O_{11}$, **Compound 9** (19 mg) was isolated as faint yellow needles, it has a negative ESI-MS analysis ($[M-H]^-$ at $m/z = 301.00627$) calculated as $C_{14}H_6O_8$. **Compound 10** (46 mg) was obtained as white crystals. It has an ESI-MS ($[M-H]^-$ at $m/z = 315.01189$), corresponding to the molecular formula of $C_{15}H_8O_8$.

2.8. Statistical analysis

Expression of data as the Mean ± SE and analysis via one-way analysis of variance followed by Tukey's test were done by using SPSS software (SPSS Inc., Chicago, IL, USA). p-value < 0.05 was considered to be statistically significant. Statistical analysis was performed with GraphPad Prism 8 software (GraphPad Software, La Jolla, California, USA).

3. Results

3.1. The in vitro antidiabetic and antioxidant activities

Both EtOH and its subfractions inhibited the activity of the tested α-amylase, β-glucosidase, and lipase enzymes (Table 1). EtOAc fraction showed the highest inhibitory activity where it showed IC_{50} values of 200.52 ± 0.87, 25.19 ± 2.65 and 22.52 ± 1.43 μg/ml for α-amylase, β-glucosidase, and lipase, respectively. The activities were comparable to the tested standard in each case (acarbose 230.85 ± 2.45, DNJ 27.72 ± 0.02, and orlistat 28.96 ± 6.4 μg/ml, respectively). Meanwhile, the MeCl and BuOH fractions showed no activity.

The highest antioxidant activity, manifested in DPPH and ORAC assays, was revealed by the EtOAc fraction with IC_{50} lower than that of BuOH and comparable to the standard Torolox (Table 1). Consequently, the EtOAc fraction was tested for the in vivo antidiabetic activity in STZ-diabetic rats. The active fraction was also subjected to UPLC-ESI-MS/MS analysis of the identification of its metabolite as well as the isolation of the major compounds.

3.2. Acute toxicity study

The results exhibited no mortality after 24 h of oral administration of EtOAc fraction in rats of both sex at graded doses up to 2 g/kg. 1/40 and 1/20 (50 & 100 mg/kg) of the maximum dose (2 g/kg) were chosen to be used for the pharmacological investigation throughout the study.

3.3. In vivo antidiabetic activity of the EtOAc fraction in STZ-diabetic rats

3.3.1. Effect on serum glucose

STZ injection-induced hyperglycemia in rats as regards to the negative control group at $p < 0.05$ (Fig. 1A). Treatment with EtOAc fraction (50 and 100 mg/kg) significantly ($P < 0.05$) decreased the serum glucose level by 63%, and 37% as compared to the STZ-diabetic group. Whereas, the ethyl acetate fraction at a dose of 50 mg/kg showed anti-hyperglycemic effect that was comparable to the standard gliclazide ($P < 0.05$). ANOVA output values: DF= 29, F= 191.6.

3.3.2. Effect on body weight

The percentage change of the final body weight (at the end of the experiment) of each group from its corresponding initial weight (before

Table 1
Results of α-amylase, β-glucosidase and pancreatic lipase inhibition activity and the in vitro antioxidant activity of *Physalis peruviana* fruits.

The tested sample	IC_{50} (μg/ml)				
	α-Amylase	β-Glucosidase	Pancreatic lipase	DPPH	ORAC
Ethanolic extract	235.0 ± 1.21	113.01 ± 4.37	145.0 ± 2.76	9 ± 1.55	8 ± 0.87
MeCl fraction	–	–	–	–	–
EtOAc fraction	200.52 ± 0.87	25.19 ± 2.65	22.52 ± 1.43	6.41 ± 0.57	6.21 ± 0.56
BuOH fraction	–	–	–	11 ± 1.4	12 ± 1.11
Acarbose	230.85 ± 2.45	–	–	–	–
1-Deoxynojrimycin	–	27.72 ± 0.02	–	–	–
Orlistat	–	–	28.96 ± 6.4		
Torolox	–	–		–	27 ± 1.41
Vitamin C	–	–		1.83 ± 0.41	–

treatment) was evaluated (Fig. 1B). In the negative control group, body weight at the end of the experiment was increased by about 14% of the initial body weight. The STZ-treated group showed highest percent decrease from its corresponding initial body weight (23%). Treatment with gliclazide, ethyl acetate fraction (50 & 100 mg/kg) decreased body weight by about 6%,8%, and 6%.

3.3.3. Effect on kidney parameters

Serum urea was significantly (at $P < 0.05$) elevated by STZ injection as compared to the negative control group (Fig. 1C). Administration of EtOAc fraction (50 and 100 mg/kg) induced a significant ((at $P < 0.05$) decrease in serum urea level by 43% and 64% as regards to STZ-diabetic group. These percentages were comparable to the standard gliclazide which achieved 67% decrease in serum urea level compared to the STZ-diabetic group. STZ significantly ($P < 0.05$) increased serum uric acid level as compared to the negative control group (Fig. 1D). ANOVA output values: DF= 29, F= 107.1.

Treatment of rats with EtOAc fraction (50 and 100 mg/kg) significantly ($P < 0.05$) decreased serum uric acid level by 61% and 49% as compared to the STZ-diabetic group. The effect of the EtOAc fraction was superior to that of gliclazide, which showed 35% decrease in serum uric acid level. ANOVA output values: DF= 29, F= 60.98.

STZ decreased albumin level by about 3 folds relative to the negative control group at $P < 0.05$ (Fig. 1E). The EtOAc fraction (50 and 100 mg/kg) increased serum albumin level by 97% and 86% as regards to STZ-diabetic group. ANOVA output values: DF = 29, F = 114.4.

The effect was comparable to gliclazide. Additionally, STZ injection significantly ($P < 0.05$) decreased the serum total protein as compared to the negative control group (Fig. 1F). Treatment with EtOAc fraction (50 and 100 mg/kg) significantly ($P < 0.05$) increased the serum total protein level by 35% and 27% compared to the STZ-diabetic group. The serum level of total protein in all treated groups was not significantly different from the negative control group and approximated the normal value. ANOVA output values: DF = 29, F = 50.22.

STZ injection significantly ($P < 0.05$) increased serum creatinine by about 4 folds as compared to the negative control group (Fig. 1G). Treatment with gliclazide and ethyl acetate fraction (50 and 100 mg/kg) significantly ($P < 0.05$) decreased serum creatinine level by 45%, 58%, and 55% as compared to STZ-diabetic group. ANOVA output values: DF = 29, F = 277.6.

3.3.4. Effect on autophagy-related indictors

Assessment of the autophagy in pancreatic and renal tissues of diabetic rats revealed that LC3II was down-regulated in STZ-diabetic group as regards the negative control group at $p < 0.05$ (Fig. 2A and B). On the other hand, it was induced successfully in the groups treated with either gliclazide or EtOAc as compared to STZ-diabetic group at $p < 0.05$ (Fig. 2A and B). ANOVA output values: DF= 29, F= 80.94 for pancreatic LC3II & DF= 29, F= 51.15 for renal LC3II.

AMPK, which induces autophagy, was significantly (at $p < 0.05$) impaired in the diabetic group as compared to the negative control. All treated groups significantly ($P < 0.05$) increased AMPK contents in pancreatic and renal tissues (Fig. 2 C and D). ANOVA output values: DF= 29, F= 80.18 for pancreatic AMPK & DF= 29, F= 73.14 for renal AMPK.

Measurement of mTOR, the major inhibitor of autophagy, revealed that its level was induced in STZ-diabetic group as compared to the negative control at $p < 0.05$. mTOR level was significantly (at $p < 0.05$) decreased upon treatment with gliclazide and EtOAc fraction in both pancreatic and renal tissues (Fig. 2E and F). ANOVA output values: DF= 29, F= 91.15 for pancreatic mTOR & DF= 29, F= 121.6 for renal mTOR.

3.3.5. Histopathological findings

Hematoxylin and eosin-stained sections of the kidney tissue from the negative control group showed a healthy appearance, with normal renal architecture formed of malpighian corpuscle which contains the glomerulus formed of capillary loops separated from Bowman capsule by Bowman Space, the proximal convoluted tubules lined by simple cuboidal with microvilli as it begins at the capsule and distal convoluted tubules (Fig. 3.A). Sections from the positive control group revealed the total absence of the glomeruli due to complete loss of capillary loops as well as the proximal and distal tubules disrupted their epithelial lining with dilated intratubular spaces (Fig. 3.B). The groups which have been treated with EtOAc fraction showed normal renal architecture appearance, especially in a higher dose (Fig. 3.D). However, hemorrhagic foci were noticed in the lower dose of EtOAc fraction (Fig. 3.C). All the previous groups were compared with the reference group that received gliclazide revealing the normal appearance of renal tissue (Fig. 3.E).

Hematoxylin and eosin-stained sections of the liver tissue from the negative control group showed the normal hepatic architecture; formed of multiple hepatic lobules. Hepatic cords are of average thickness radiating centrally from the central vein to the portal area (Fig. 3.A). Sections from the positive control group showed signs of degenerated hepatocytes with ruptured cell membranes, also some with karyolysis nuclei and others with pyknotic nuclei, the central vein was dilated and congested with activated kupffer cells (Fig. 3.B). On the other hand, the groups which received the EtOAc fraction in the tested doses showed almost normal appearance of hepatic tissue unless the inflammatory cells around the central vein (Fig. 3.C and D). All the groups were compared to gliclazide showing normal appearance of hepatic cords with average thickness except for the dilated congested sinusoids (Fig. 3. E).

The histological examination of pancreatic tissues of all the examined groups revealed that the negative control group has normal architecture: formed of endocrine portion (islets of Langerhans) and exocrine pancreas in the form of acini with average-thickness pancreatic vessels (Fig. 3.A). The positive control group that received STZ showed destructive changes as regards to the endocrine pancreas in form of islets of Langerhans with widening intercellular spaces, the endocrinocytes showing signs of degeneration with a decrease in their number and shrunken the islet area with irregular outlines the exocrine pancreas revealed dilated acini with flattened their nuclei (Fig. 3.B). The groups which were treated with the EtOAc fraction showed gradual

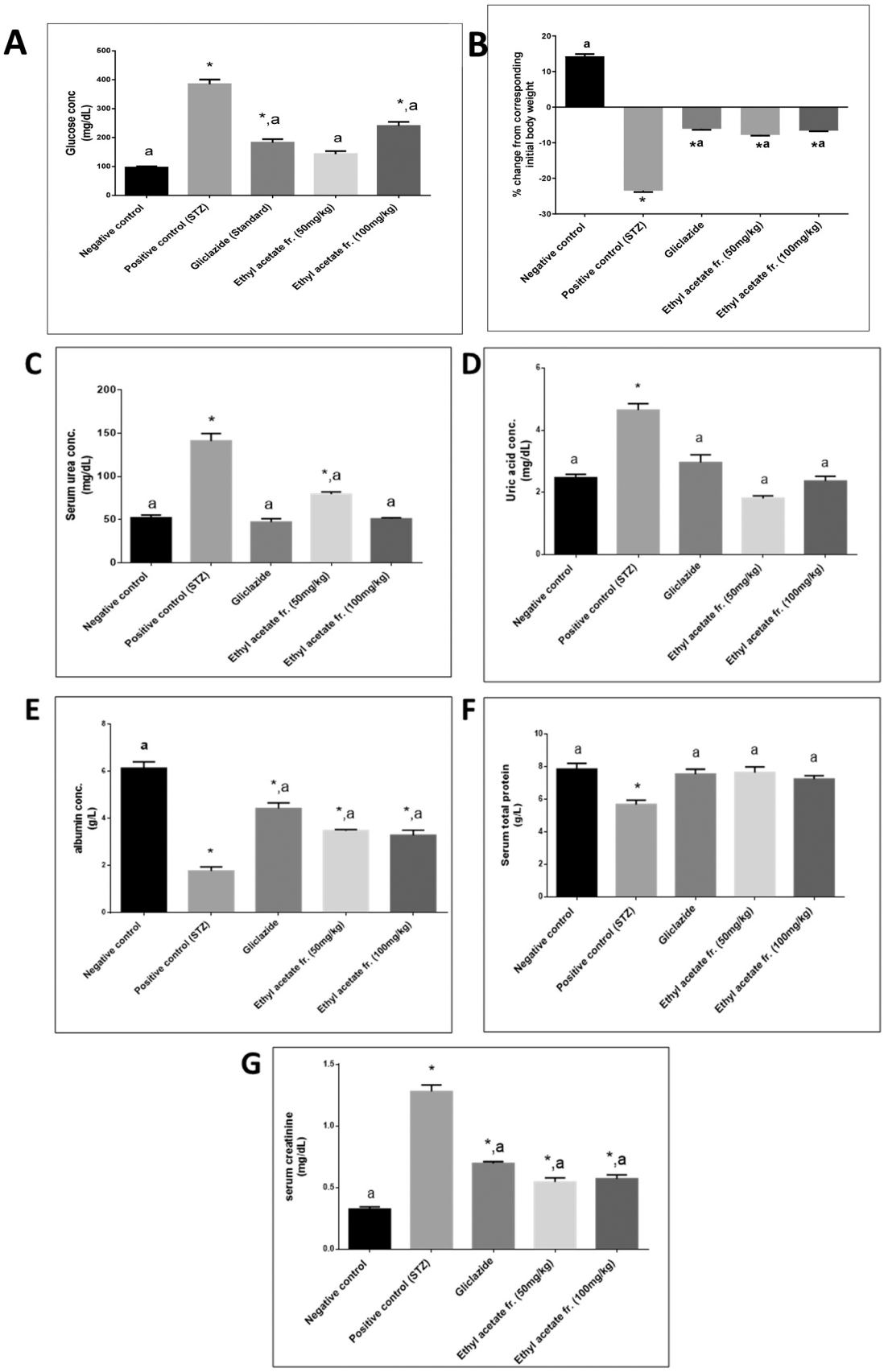

Fig. 1. Effect of the ethyl acetate fraction of *Physalis peruviana* fruits on: A: serum glucose; B: percent change from corresponding body weight C: serum urea, D: effect on uric acid, E: albumin, F: serum total protein, G: serum creatinine**.** Each value represents mean ± SEM (n = 6). Statistical analysis was carried out by One-way ANOVA followed by Tukey post hoc test. *Significantly different form negative control. [a] significantly different from positive control (STZ) at $p < 0.05$.

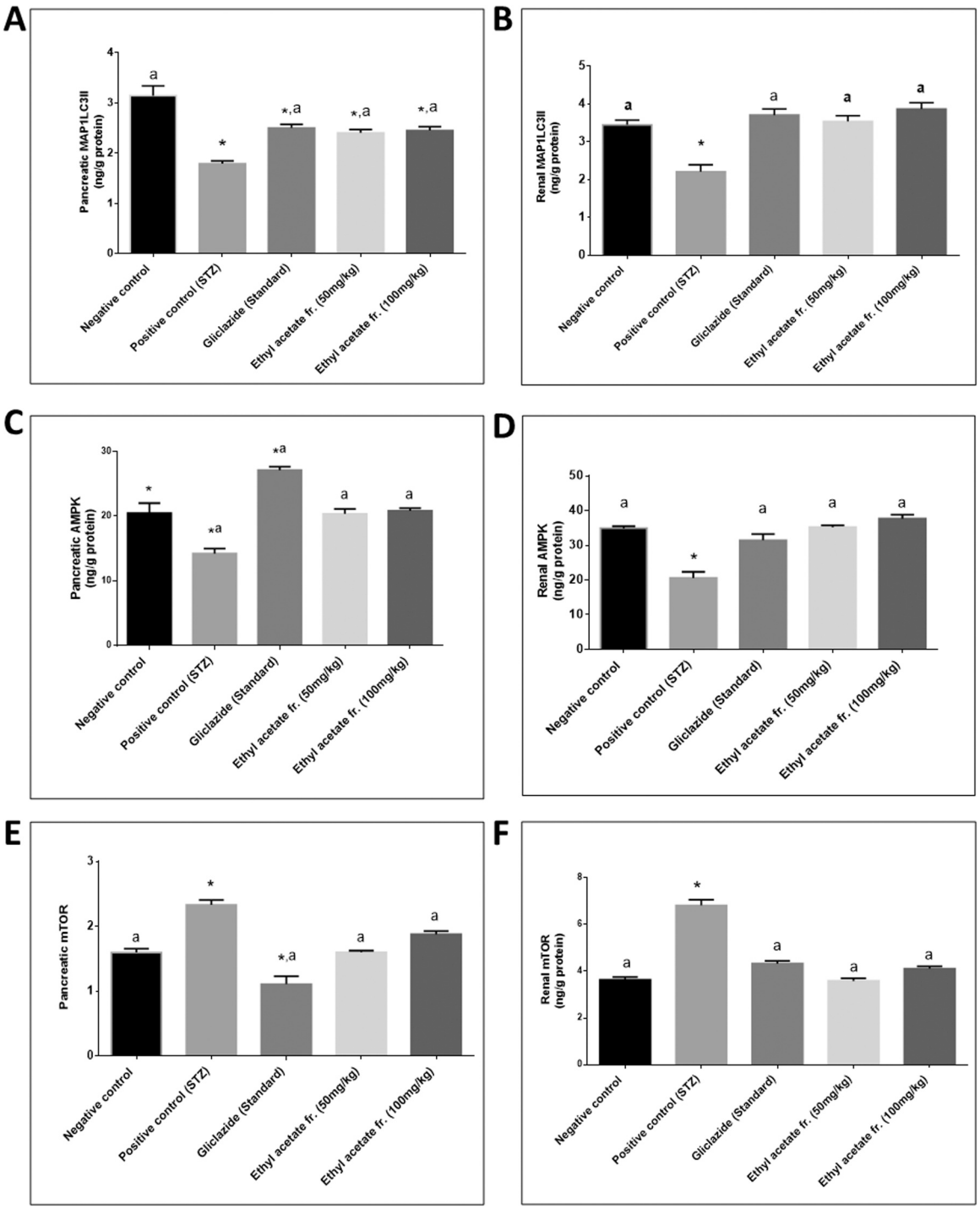

Fig. 2. Effect of the ethyl acetate fraction of *Physalis peruviana* fruits on: A: MAP1LC3II in pancreatic tissues, B: MAP1LC3II in renal tissues, C: AMPK in pancreatic tissues, D: AMPK in renal tissues, E: mTOR in pancreatic tissues, F: mTOR in renal tissues. Each value represents mean ± SEM (n = 6). Statistical analysis was carried out by One-way ANOVA followed by Tukey post hoc test. *Significantly different form negative control. [a]significantly different from positive control (STZ) at $p < 0.05$.

improvement in the number of endocrinocytes and the roundness of islet itself with increased dose (Fig. 3.C and D). The gliclazide group has a normal pancreatic architecture appearance (Fig. 3.E).

3.3.6. *Histochemical expression of PAS*

Histomorphometric analysis was achieved to determine the content of glycogen in the kidney, liver, and pancreatic tissues for all tested groups (Fig. 4), where the positive control recorded the highest level in kidney tissues. Treatment with EtOAc fraction (100 mg/kg) showed a better effect as compared to the reference group. Sections from the liver tissues, stained with Periodic acid Schiff stain (PAS), revealed the highest content of glycogen in the positive control group. On the other hand, the group treated with EtOAc fraction (50 mg/kg) showed a slight improvement in the glycogen content in the hepatocytes in between the congested sinusoids. Interestingly, the group treated with EtOAc at a higher dose (100 mg/kg) showed marked improvement in mucopolysaccharide content of hepatocytes except for some cells around the central vein. The treatment with EtOAc fraction also resulted in a

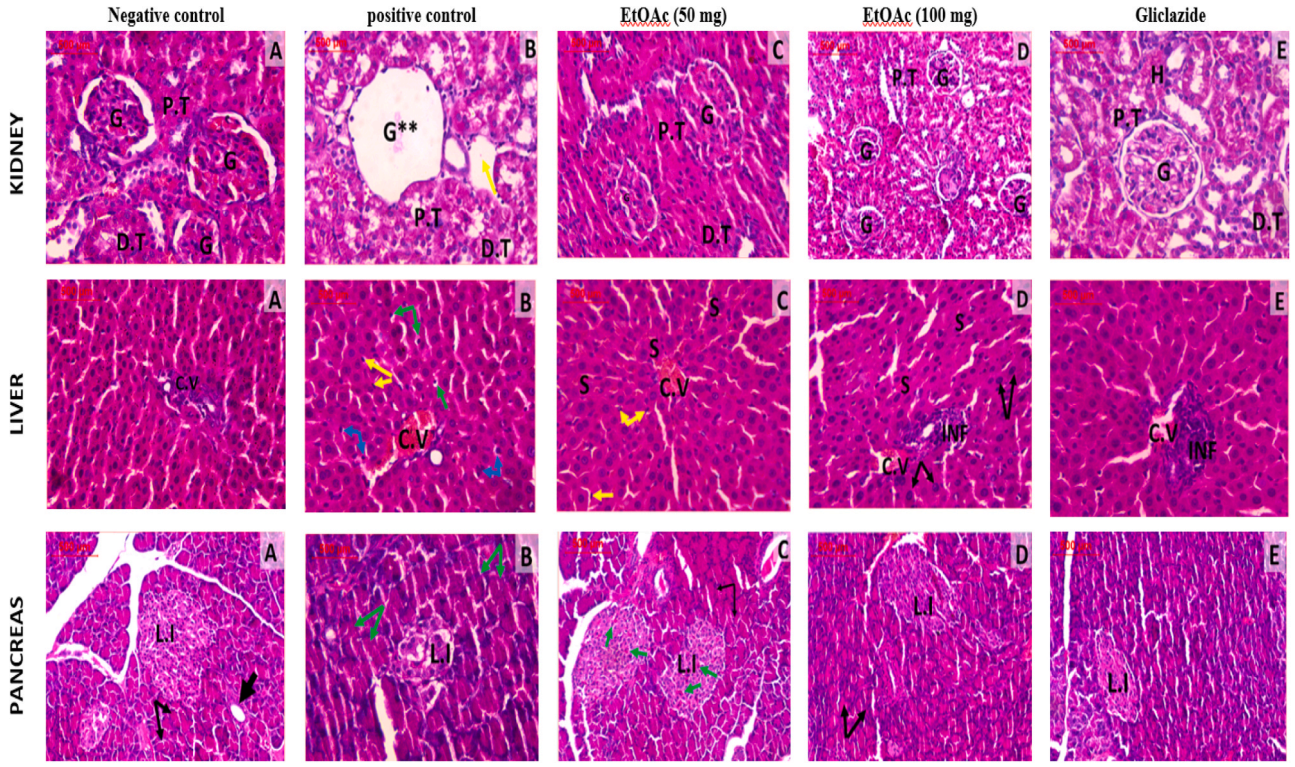

Fig. 3. A photomicrography of kidney, liver and pancreatic tissues from all tested groups: A) Negative control, B) positive control, C) EtOAc (50 mg), D) EtOAc (100 mg), E) Gliclazide. Kidney sections showing: G; Normal glomeruli, G* *; Lost glomeruli capillaries, P.T; Proximal tubules, D.T; Distal tubules, H; Hemorrhagic foci, Yellow Arrows; Dilated intratubular spaces (H&E 400x). Liver sections showing: C.V; Central vein, S; Dilated congested sinusoids, INF; Inflammatory cells, Blue Arrows; hepatocytes with Karyolysis nuclei, Green Arrows; Hepatocytes with pyknotic nuclei, Yellow Arrows; Kupffer cells, Black Arrows; Regenerated hepatocytes (H&E 400x). Pancreatic sections showing: L.I; Islets of Langerhans, Black Thick Arrows; Pancreatic vessels, Black Thin Arrows; Pancreatic acini, Green Arrows; Hyalinized strains (H&E 400x).

significant reduction of the glycogen content from the pancreatic cells. Noticeable improvement was also recorded at the higher dose of the EtOAc fraction (100 mg/kg) as compared to the reference group.

3.3.7. *Immunohistochemical expression of P53*

Immunomorphometric analysis was performed to determine the extent of damage in renal tissue quantitatively. The results ascertained that the area of the damage was significantly greater in the positive control group (Fig. 5). Treatment with EtOAc fraction leads to a significant reduction of tissue damage, especially at higher doses.

P53 expression was almost undetectable in the hepatic tissue of the normal control group. In the positive control group, strong P53 immunostaining was observed, which was significantly reduced upon treatment with EtOAc fraction compared to the reference drug.

The immunohistochemistry staining of the pancreatic tissues from the positive control group showed a significant increase of p53 as regards the negative control. On the other hand, the expressions of p53 from positively stained pancreatic cells were reduced when the animals were treated with EtOAc fraction, whereas P53 expression depicted a marked significant decrease with higher doses of EtOAc fraction (Fig. 5).

3.4. *UPLC-ESI-MS/MS analysis for the identification of metabolites from the EtOAc fraction*

UPLC-ESI-MS/MS analysis was applied for secondary metabolites profiling of the bioactive ethyl acetate fraction (EtOAc) in both positive and negative ion modes (Fig. 6), which led to the identification of nineteen compounds (Table 2). Among the identified compounds, four flavonoid aglycones viz. quercetin, kaempferol, myricetin hexamethyl ether and 3,5,7,2′,6′-pentamethoxyflavone; four flavonoid glycosides viz. quercetin-3-arabinoside-7-glucoside, quercetin-3-*O*-monohexoside, kaempferol-3-*O*-monohexoside and quercetin-3-*O*-rhamnoside. Five gallotannin derivatives which included 6-methyl 2-galloylgalactarate, two digalloyl glucose isomers, dimethyl 2-galloylgalactarate and epigallocatechin gallate. In addition to gallic acid, ellagic acid and methylellagic acid, as well as two phenolic acids 1-*O*-sinapoylglucose and di-*O*-caffeoylquinic acid.

A dicaffoeylquinic acid was detected at Rt 1.09 min with molecular ion peak $[M\text{-}H]^-$ of *m/z* 515.12518 was calculated as $C_{25}H_{24}O_{12}$ and daughter ion at *m/z* 353 due to the loss of one caffeoyl fragment as well as *m/z* 191 (deprotonated quinic acid moiety), 179 (deprotonated caffeic acid moiety) and 173. So, peak 2 was identified as di-*O*-caffeoylquinic acid [47].

At Rt 3.07, a peak with molecular ion $[M\text{-}H]^-$ at *m/z* 595.11322 calculated for the neutral formula $C_{26}H_{28}O_{16}$ which showed fragment ions at *m/z* 433 [M - H - 162]-, due to the loss of a hexose from position 7, which is easy to lose and a fragment ion at *m/z* 301 [M - H −162–132]- indicating the loss of a pentose from the 3-*O*-position and the presence of a quercetin aglycone, so it was identified as quercetin 3-pentoside 7-hexoside [48]. Peak 7 (Rt 3.18 min) with the molecular ion of $[M\text{-}H]^-$ at *m/z* 463.98956 and $[M+H]^+$ at *m/z* 465.98956 calculated for the neutral formula $C_{21}H_{20}O_{12}$, yielding a fragment ion of *m/z* 301 [M - H - 162]-, assigned to a quercetin aglycone with a loss of 162 amu (a hexose moiety), and was tentatively identified as quercetin-3-*O*-hexoside. Peak 11 at Rt 5.44 min, showed a molecular ion peak $[M+H]^+$ at *m/z* 449.02145, calculated for the neutral formula $C_{21}H_{20}O_{11}$ which produced a fragment ion of 303 [M+H-146] indicated the presence of quercetin as an aglycone after the loss of a rhamnose moiety, this compound was identified as quercetin-3-*O*-rhamnoside [49]. Peak 10 (Rt 4.57 min) showed a molecular ion $[M\text{-}H]^-$ at *m/z* 447.10817 and $[M+H]^+$ at *m/z* 449.10818 calculated as neutral formula $C_{21}H_{20}O_{11}$, this produced a fragment ion of *m/z* 285 [M-H-162], identified as kaempferol aglycone

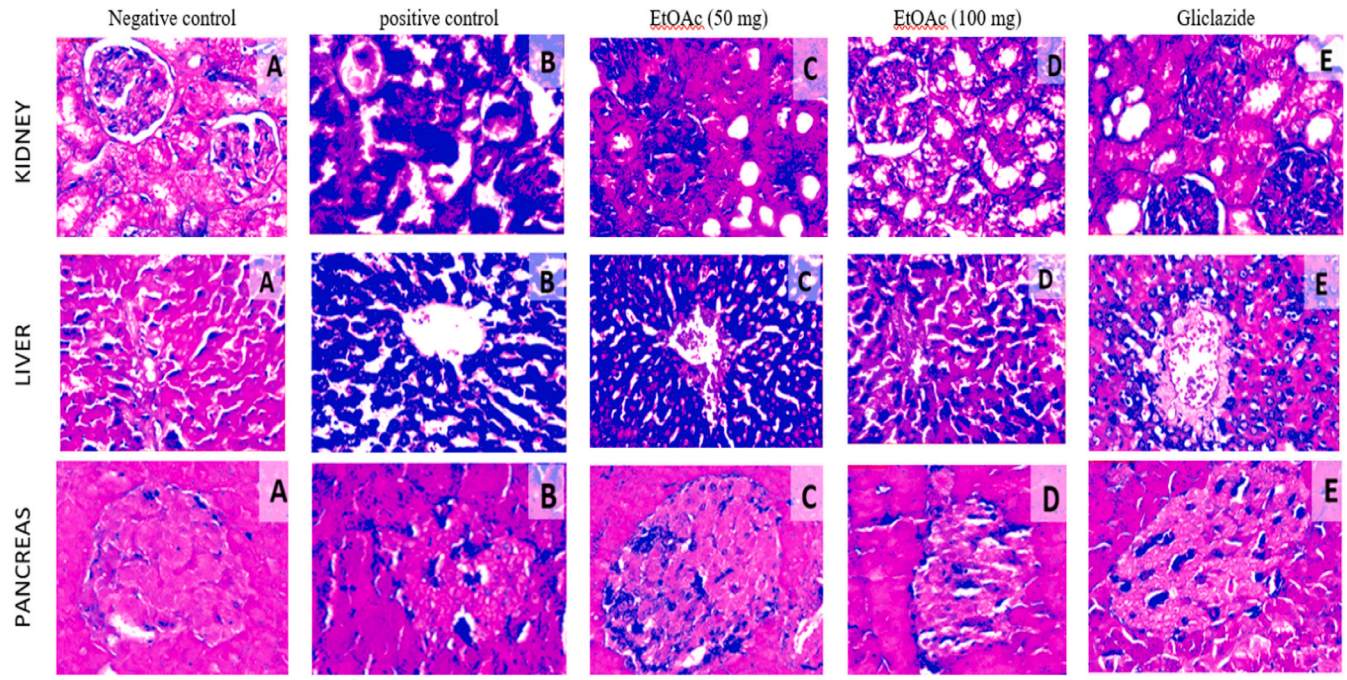

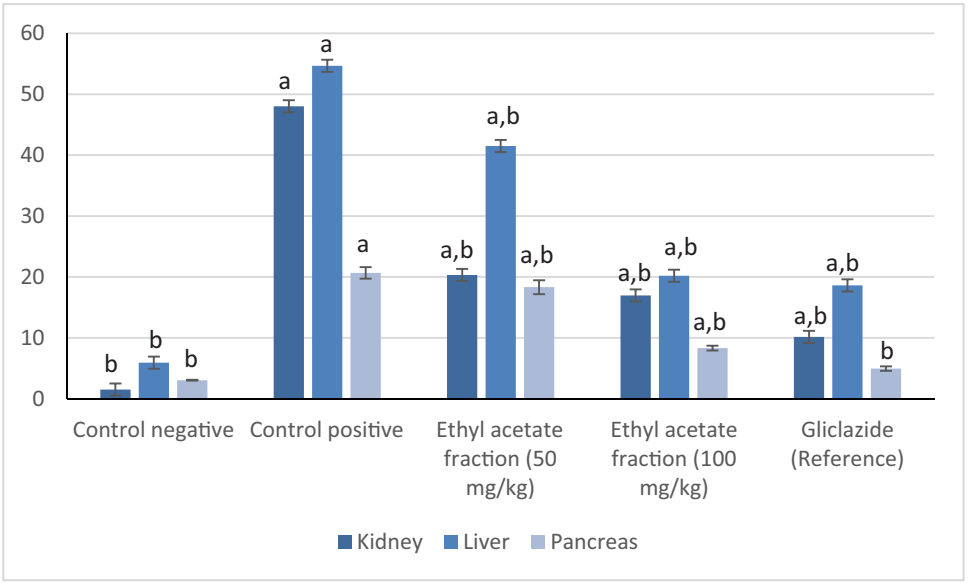

F

Fig. 4. A Binary image taken by the image analysis system of kidney, liver and pancreatic tissue showing glycogen content expressed by PAS stain, detected by blue color highlighted the positive cells to be measured as area percent in all tested groups: A) Negative control, B) positive control, C) EtOAc (50 mg), D) EtOAc (100 mg), E) Gliclazide. (PAS 200x), F) Area of glycogen % in kidney, liver, pancreatic tissues detected by PAS stain. Data were expressed as Mean ± SE (n = 6). Statistical analysis was carried out by one-way ANOVA using Tukey as post-hoc test. [a] Significantly different from Control negative at $P < 0.05$. [b] Significantly different from Control positive at $P < 0.05$.

after the loss of a hexose moiety with 162 amu, so this compound was identified as kaempferol-hexoside [49]. Peak 16 (Rt 7.53 min) with a molecular ion $[M-H]^-$ at *m/z* 301.0354 and $[M+H]^+$ at *m/z* 303.0496 calculated as neutral formula $C_{15}H_{10}O_7$ identified as quercetin aglycone, with 2 daughter ions at *m/z* 273 $[M-H- CO]^-$ and 257 $[M-H-CO2]^-$ [49]. Similarly, peak 17 at Rt 9.14 min showed $[M-H]^-$ at *m/z* 285.0406 and $[M+H]^+$ at *m/z* 287.05484 calculated for the neutral molecular formula $C_{15}H_{10}O_6$ which was identified as kaempferol aglycone [49].

Peak 15 at Rt 6.05 min showed a molecular ion peak $[M+H]^+$ at *m/z* 303.00627 and $[M-H]^-$ at *m/z* 301.09527 fragment ions at *m/z* 257, 229, and 185, characteristic fragments of ellagic acid, similarly, peak 12 at Rt 5.60 with $[M-H]^-$ at *m/z* 315.01189 and $[M+H]^+$ at *m/z* 317.02192 calculated for the neutral molecular formula $C_{15}H_8O_8$ which showed the same fragmentation pattern as ellagic acid with the presence of a CH_3 moiety was identified as Methyl-ellagic acid [50]. Peak 13 at Rt 5.67 with molecular ion peak $[M-H]^-$ at *m/z* 385.11429 calculated for the molecular neutral formula $C_{17}H_{20}O_{10}$ and a daughter ion at 223 [M-H-162]- indicated the presence of sinapic acid aglycone which lost a glucose moiety, so this peak was identified as 1-*O*-Sinapoylglucose [51].

Concerning the gallotannins, peak 4 (Rt 1.46 min) and 9 (4.33 min) were identified as two isomers of digalloyl glucosides, as they had $[M-H]^-$ at *m/z* 483.08691 calculated for the neutral formula $C_{20}H_{20}O_{14}$ with

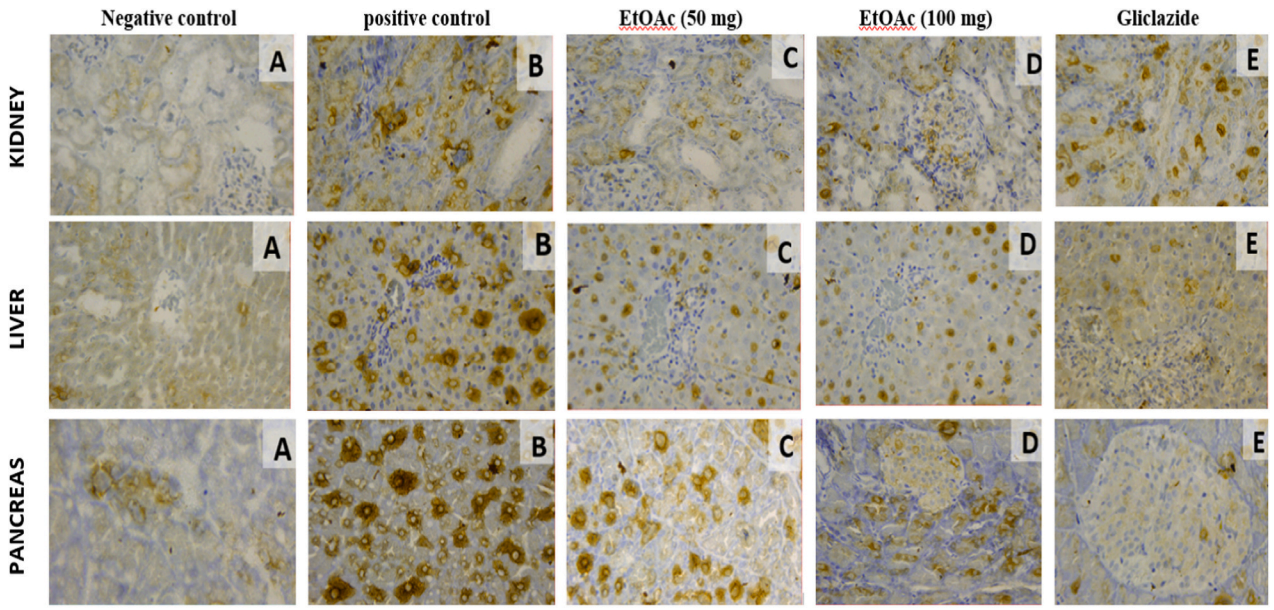

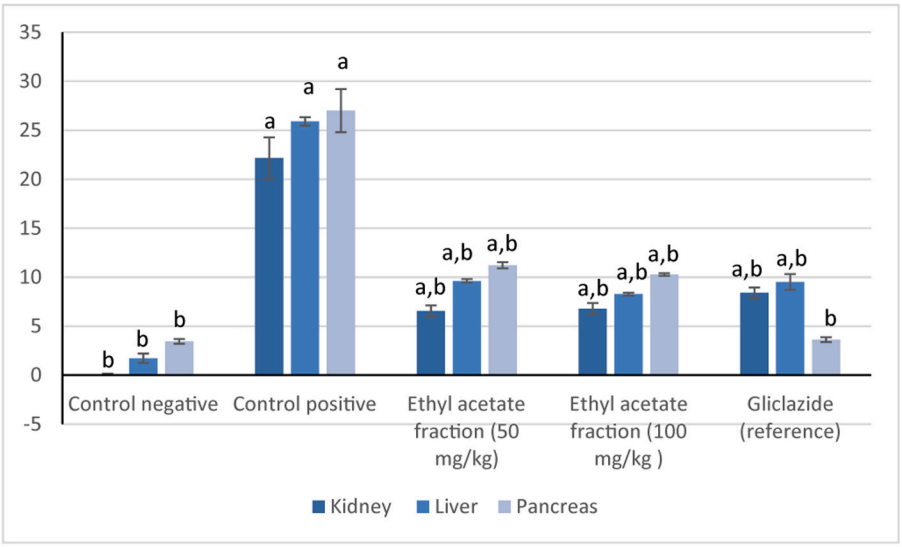

F

Fig. 5. A photomicrography of kidney, liver and pancreatic tissues showing expression of P53 in all tested groups: A) Negative control, B) positive control, C) EtOAc (50 mg), D) EtOAc (100 mg), E) Gliclazide. As the highest expression were be noticed in Group B, to be decreased gradually in Group C&D respectively when compared with the control group and reference group; Group E (P53 200x). F) Area % of P53 immuno-histochemical expression in kidney, liver, pancreatic tissues. Data were expressed as Mean ± SE (n = 6). Statistical analysis was carried out by one-way ANOVA using Tukey as post-hoc test. [a] Significantly different from Control negative at $P < 0.05$. [b] Significantly different from Control positive at $P < 0.05$.

characteristic fragment ions at *m/z* 313 [M−H−gallic acid]$^-$ ion as well as with *m/z* 169 [gallic acid-H]$^-$ and 125 [gallic acid−H−COO]$^-$[52]. In addition to peak 14 at Rt 5.84 with [M-H]$^-$ at *m/z* 457.0779 and characteristic fragment ions of *m/z* 331, 305, 287,192,169, this was identified as Epigallocatechin Gallate (EGCG) [53].

3.5. Isolation of EtOAc major compounds and in vitro antidiabetic assay of the isolated compounds

Upon applying column chromatographic fractionation technique on the bioactive EtOAc fraction, ten compounds (1−10) were isolated and identified using various spectral analysis & their activity was measured by Biochemical *In vitro* assays: Enzyme inhibition assays (Fig. S1(A, B & C) .Tables S1 and S2) reveal the chromatographic behavior, UV spectra, ESI-MS (negative mode), ^{1}H and ^{13}C NMR data of the isolated copmpounds which were consistent with those previously reported for, 2,6-di-*O*-galloyl-(*α/β*)-$^4C_1$- glucopyranose 1 [54]; kaempferol 3-*O*-galactoside 2 [55]; quercetin 3-*O*-galactoside 3 [56], gallic acid 4 [57]; 2,3-di-*O*-galloyl-(α/β)-$^4C_1$-glucopyranose or nilocitin 5 [58]; quercetin 6 [54]; kaempferol 7 [59]; quercetin 3-*O*- rhamnoside 8 [54], ellagic acid 9 [57]; 3-*O*-methylellagic acid **10** [60]. Table 3 showed that all the isolated compounds (1−10) have inhibitory activity on *α*-amyase, *β*-glucosidases, and pancreatic lipase enzymes. It is noteworthy that compounds 3, 4, 8, and 10 were the most active in comparison to the standard drugs.

4. Discussion

Diabetes mellitus is a growing serious disease worldwide which constitutes an alarming situation. In the year 2018, WHO reported that

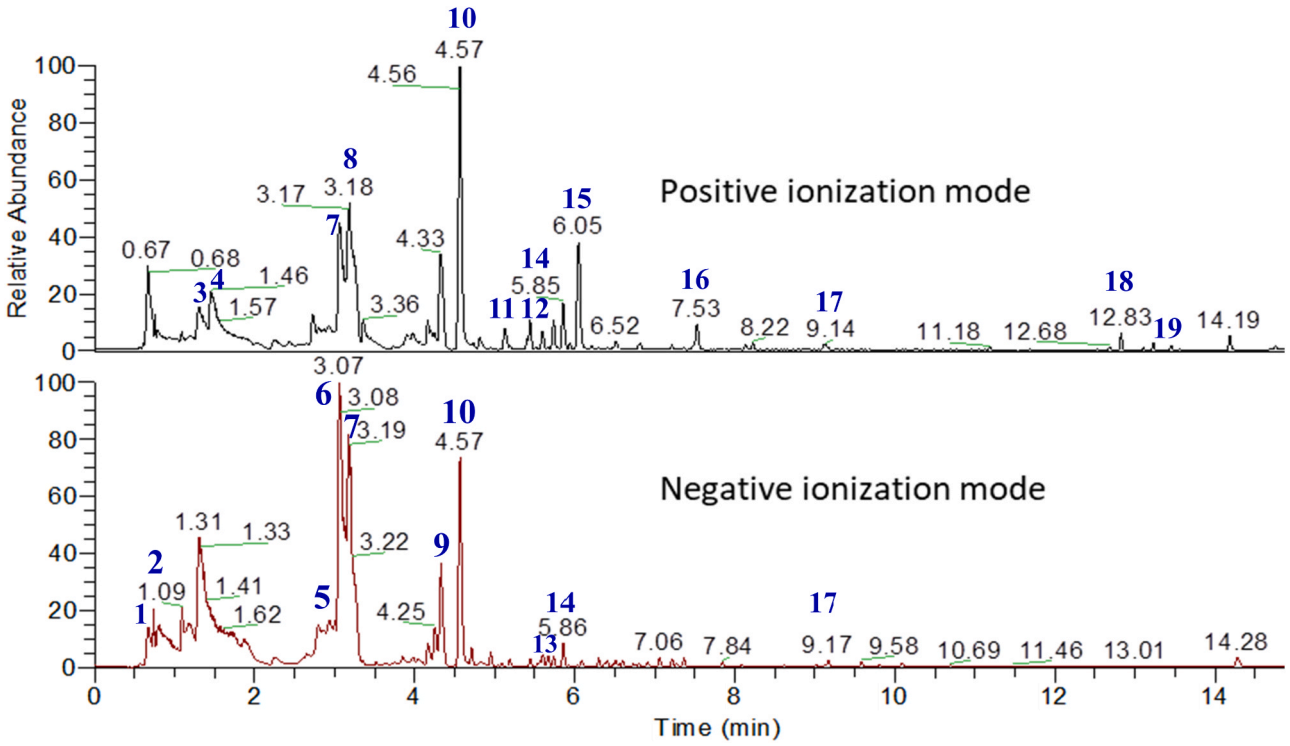

Fig. 6. Base peak chromatograms (BPC) of the ethyl acetate fraction of *Physalis peruviana* fruits measured in positive and negative ionization modes.

Table 2
The major compounds identified compounds from the ethyl acetate fraction of *Physalis peruviana* fruits.

Peak no.	RT	$[M-H]^-$	$[M+H]^+$	Neutral Formula	rdb	Error	Mass fragmentation	The identified compound
1	0.74	341.10880		$C_{12}H_{22}O_{11}$	2.5	2.8	179,191,225	Mannobiose
2	1.09	515.12518		$C_{25}H_{24}O_{12}$	14.5	13.1	111,173,191	Di-O-caffeoylquinic acid
3	1.30		377.06833	$C_{14}H_{16}O_{12}$	6.5	-8.28	97,129,139,145,215,288,319,337	6-Methyl 2-galloylgalactarate
4	1.46	483.08691	485.13248	$C_{20}H_{20}O_{14}$	10.5	-11.6	313, 169,125	Digalloyl glucose isomer 1
5	2.87	169.01319		$C_7H_6O_5$	5.5	-2.96	125,07, 97	Gallic acid
6	3.07	595.12322		$C_{26}H_{28}O_{16}$	13.5	-11.25	433, 301, 162,135	Quercetin 3-pentoside 7-hexoside
7	3.18	463.08956	465.08956	$C_{21}H_{20}O_{12}$	13.5	4.11	301	Quercetin-3-O-monohexoside
8	3.18		391.08398	$C_{22}H_{14}O_7$	6.5	-7.9	136,268	Dimethyl 2-galloylgalactarate
9	4.33	483.08691	485.08691	$C_{20}H_{20}O_{14}$	10.5	-11.6	313, 169,125	Digalloyl glucose isomer 2
10	4.57	447.10817	449.10818	$C_{21}H_{20}O_{11}$	11.5	-10.9	285	Kaempferol-3-*O*-monohexoside
11	5.44	447.00123	449.02145	$C_{21}H_{20}O_{11}$	12.5	-10.7	303	Quercetin-3-*O*-rhamnoside
12	5.60	315.01189	317.02192	$C_{15}H_8O_8$	7.5	3.2	257, 185	Methyl-ellagic acid
13	5.67	385.11429		$C_{17}H_{21}O_{10}$	7.5	3.5	223, 162	1-*O*-Sinapoylglucose
14	5.84	457.0779	459.09155	$C_{22}H_{18}O_{11}$	13.5	-1.3	331, 305, 287,192,169	Epigallocatechin Gallate
15	6.05	301. 09527	303.00627	$C_{14}H_6O_8$	11.5	3.8	257, 229, 185	Ellagic acid
16	7.53	301.0354	303.0496	$C_{15}H_{10}O_7$	11.5	3.72	301, 273,257	Quercetin
17	9.14	285.0406	287.05484	$C_{15}H_{10}O_6$	11.5	4.1	133	Kaempferol
18	12.83		403.13806	$C_{21}H_{22}O_8$	10.5	-1.6	183,211,301,358,373	Myricetin hexamethyl ether
19	13.23		373.12781	$C_{20}H_{20}O_7$	10.5	-0.9	183,211,271,300,343	Pentamethoxyflavone

about 4.22 billion population worldwide suffer from diabetes and that 4.18 billion will be affected soon [61]. α-Amylase is a pancreatic enzyme that hydrolyzes starch and glycogen, while the glucosidase enzyme is an enzyme located in the brush-border surface membrane of the small intestine that hydrolyzes various carbohydrates to glucose [62]. The whole process of hydrolysis of carbohydrates increases after the meal; an increase in blood glucose level known as postprandial hyperglycemia [63]. Post-prandial hyperglycemia causes vascular complications like nephropathy, neuropathy, retinopathy in addition to the damage of vital organs [64]. Moreover, inhibition of fat digestion through repression of the pancreatic lipase activity was proved to exacerbate postprandial glycemia by increasing the gastric emptying rate and reducing incretin response [65]. One of the therapeutic targets to treat diabetes and its complications is the retardation of glucose and lipid absorption through the inhibition of lipid and carbohydrates hydrolyzing enzymes, i.e., pancreatic α-amylase and lipase as well as the intestinal glucosidase. The inhibition of their activity is an important therapeutic strategy for the treatment of diabetes and controlling its compilations. The commercial drugs such as acarbose, voglibose, and miglitol, which are used for the management of type-2 diabetes, have been reported to have adverse effects like abdominal distension, bowel disruption, and diarrhea [61]. Therefore, there is always a need for drug discovery of natural products that can act as amylase and glucosidase inhibitors.

Fortunately, the EtOH extract of the fruits of *P. peruviana* L as well as its EtOAc fraction inhibited α-amylase, β-glucosidase as well as pancreatic lipase enzymes where EtOAc showed promising activities in regards to the tested standards. Moreover, EtOH and EtOAc showed strong antioxidant activity which contributes to their antidiabetic action through free radical scavenging and reducing the oxidative stress caused by hyperglycemia. Accordingly, EtOAc fraction was selected for further

Table 3
α-Amylase, β–glucosidase, pancreatic lipase and the in vitro antioxidant activity of the isolated compounds from the EtOAc fraction of *Physalis peruviana* fruits.

The tested compounds	α-Amylase IC_{50} (μg/ml)	β-Glucosidase	Pancreatic lipase	DPPH	ORAC
1	470.25 ± 4.8	6.9 ± 3.3	1.97 ± 1.8	3.53 ± 1.22	3.40 ± 1.16
2	478 ± 5.7	5.4 ± 2.8	1.99 ± 1.4	10.26 ± 1.27	10.52 ± 2.22
3	224.44 ± 4.2	3.5 ± 2.1	1.94 ± 1.5	11.89 ± 1.73	12.05 ± 2.69
4	184.1 ± 3.8	4.3 ± 2.2	1.98 ± 1.6	77.45 ± 1.42	77.01 ± 2.33
5	472.3 ± 6.8	7.2 ± 3.3	2.3 ± 1.7	2.01 ± 2.58	1.98 ± 2.55
6	547.04 ± 10.2	–	12.99 ± 3.9	6.29 ± 1.46	7.21 ± 152
7	662.49 ± 7.8	374.26 ± 7.8	22.46 ± 1.5	15.0 ± 0.43	16.0 ± 0.38
8	186 ± 4.1	5.5 ± 2.1	2.1 ± 1.8	23.02 ± 1.52	23.27 ± 1.46
9	294.8 ± 8.4	803.98 ± 7.26	24.51 ± 2.2	13.0 ± 2.75	12.0 ± 0.89
10	188 ± 2.8	6.1 ± 2.8	2.2 ± 1.3	5.31 ± 1.35	5.67 ± 2.06
Acarbose	230.85 ± 2.45	–	–	–	–
1-Deoxynojrimycin	–	27.72 ± 0.02	–	–	–
Orlistat	–	–	28.96 ± 6.4	–	–
Torolox	–	–	–	–	27 ± 1.41
Vitamin C	–	–	–	1.83 ± 0.41	–

in vivo testing as well as metabolic profiling.

STZ-induced diabetic animal models are useful platforms for triggering hyperglycemia [66]. STZ induces an autoimmune process that destroys pancreatic *β* cells bringing about degranulation and loss of the ability to secrete insulin [67,68]. Thus, in the present investigation, STZ was utilized for valid induction of diabetes in rats. Injection of STZ caused an increment in blood glucose level which was restored to the normal level upon treatment with the EtOAc fraction. Diabetic animals also showed an obvious reduction in their body weight. The animals became unable to metabolize carbohydrate fuel sources and this lead to a shift in reliance to fatty fuels resulting in wasting fat stores and loss of weight as reported previously [69]. EtOAc fraction lowered the plasma glucose level concurrently with stimulation of weight gain in STZ-diabetic rats. This antihyperglycemic effect was comparable with that of gliclazide, the standard drug. Gliclazide is known to produce antihyperglycemic effect via pancreatic (through blocking K^+ channels in the pancreatic *β* cells and thus stimulating insulin secretion) or extra pancreatic (by increasing tissue uptake of glucose) mechanisms [70,71]. Hence, it could be assumed that the EtOAc fraction of *P. peruviana L* produces similar effects like gliclazide. This antihyperglycemic effect of the EtOAc fraction was associated with improved histopathological features in pancreatic, renal and hepatic tissues of diabetic animals.

Uncontrolled hyperglycemia in diabetic patients usually results in several diabetic complications including nephropathy, neuropathy, and retinopathy. Diabetic nephropathy is a serious complication of diabetes (type 1 and type 2) which leads to end-stage renal disease in 30% of individuals with diabetes. This complication is evolved due to functional derangement and structural remodeling of the kidney which are triggered by hyperglycemic injury. These are linked to different signaling pathways interacting and resulting in the major pathogenic features of DN including mesangial expansion, oxidative stress, glomerular hypertrophy, tubular inflammation, and renal fibrosis [72].

These progressions are attributed to constant hyperglycemia and expanded levels of BUN, creatinine, urea and uric acid as shown in the present study in STZ-diabetic rats. Clinically, the increment in blood urea level concomitantly with elevated blood sugar indicates damage to the kidney of diabetic patients [73]. This is in agreement with other experimental studies that showed increased urea and serum creatinine in diabetic rats referring to progressive renal damage [74]. The elevation in kidney parameters was accompanied by the reduced serum levels of total protein and albumin. Hypoalbuminemia is of important clinical significance as it was correlated with reduced kidney function as well as poor renal prognosis in patients with diabetic nephropathy [75]. Treatment of diabetic rats with *P. peruviana* EtOAc fraction significantly diminished the levels of urea, uric acid, creatinine, BUN demonstrating their expanded freedom from the kidney. Furthermore, the EtOAc fraction restored the kidney function by elevating the reduced serum total protein and albumin levels. Similar findings were reported regarding the renoprotective effect of *P. peruviana*, however, in normal not diabetic rats [76]. The golden berry EtOAc fraction was previously reported to protect against acute renal injury induced by cisplatin and improved kidney histology [76]. Similarly, in the current work, EtOAc fraction of *P. peruviana* ameliorated histopathogical derangement in the diabetic kidney, pancreas and had almost normally appearance of renal architecture. The EtOAc fraction not only improved diabetic nephropathy, but also decreased histological alterations in liver tissue. The hepatoprotective and renoprotective effects of *P. peruviana* extract including its antioxidant and antifibrotic mechanisms were previously reported [77]. In addition, a recent study has shown that *P. peruviana* prevent hepatic lipoperoxidation in high fat diet-induced obese mice [78].

Periodic acid Schiff (PAS) is a special stain that shows detailed cellular structure and staining of structures that contain a high proportion of carbohydrate macromolecules such as glycogen. Diabetic rat kidneys demonstrated thickening of the glomerular basement membrane and a narrow renal tubular lumen, consistent with previous studies [79]. In contrast, the kidney morphology of the treated animals showed a reduction in the extent of glomerular hypertrophy. Glycogen is the primary storage form of glucose and is known to increase intracellularly in diabetics due to mucin and formation of glycoconjugate [80]. Diabetic rat liver also showed an increment in the glycogen deposition. The glycogen accumulation indicates severe hyperglycemia so it is referred to as a glycogenic hepatopathy [81].

Apoptosis is a process of programmed cell death and presented by internucleosomal cleavage of DNA, cell surface blebbing, and formation of apoptotic bodies. Apoptosis in Islet *β* cells occurs especially in immune-mediated diabetes by the effect of membrane-bound death signaling molecules like interleukin1-β, TNF-α, and IFN-γ [82]. In the present study, STZ-diabetic rats showed elevated expression of P53, an important apoptotic mediator, in pancreatic, renal, and hepatic tissues as well. In parallel, previous studies showed increased *β* cell apoptosis as a dominant source of *β* cell replenishment in type 1 diabetic patients [83,84]. If this increased apoptosis could be targeted and controlled, the regeneration of *β* cell mass and return of function might be accomplished. Apoptosis is an important factor for the progression of DN as it participates in podocyte injury [85]. Previous studies have explored the role of renal expressions of p53, caspase-3, and Bcl-2 in the progression of DN [86]. Treatment with EtOAc of *P. peruviana* L. improved the induction of apoptosis in pancreatic, renal, and hepatic tissues as referred from decreased expression of P53. Likewise, studies have shown the anti-apoptotic mechanism of *P. peruviana* in the treatment of carcinoma-induced hepatic damage via downregulation of p53 expression and up-regulation of Bcl2 [87]. It also increased the expression of Bcl-2 protein in hepatic and renal tissues in $CdCl_2$ rats [88]. Hence, it is

suggested that the EtOAc fraction reduced apoptosis in pancreatic tissue to allow replenishment of β cells. Moreover, it could protect against diabetic complications like nephropathy and hepatic damage via its apoptotic action besides its anti-hyperglycemic effect.

Conventional biomarkers for the detection and prediction of DN have several limitations. Novel biomarkers have been evolved recently which have higher sensitivity and specificity for earlier detection of DN [89]. In the present study, indicators of autophagy such as light chain 3II (LC3II), AMP-activated protein kinase (AMPK), and mammalian target of rapamycin (mTOR) were assessed. These parameters were disrupted and correlated with the presence of hyperglycemia and the worsening of renal function tests in diabetic rats. This is consistent with previous studies [90]. LC3 is the most important reliable marker of autophagy. The conversion of LC3I to LC3II is closely correlated with the extent of autophagosome formation. So, LC3II is the main marker that reflects the level of autophagy [91]. During the formation of autophagosomes, LC3 is lipidated. This LC3-phospholipid conjugate (LC3-II) is accumulated in autophagosomes and autolysosomes. In our findings, EtOAc fraction effectively increased the level of LC3II, suggesting that the EtOAc fraction could prevent diabetic nephropathy via triggering autophagy.

AMPK-mTOR signaling pathway has been recently recognized to regulate autophagy [92]. AMPK is an important serine/threonine protein kinase that is activated under energy-depleted conditions and is likely to be suppressed in diabetic nephropathy. Investigations using diabetic animal models have reported the inactivation of AMPK (decreased phosphorylation) takes place in renal glomeruli and tubules [93]. AMPK also induces autophagy through inhibition of mTORC1 activity via phosphorylation of its regulatory-associated proteins [94, 95]. Hyperactivation of the mTOR pathway in diabetic nephropathy plays a central role in kidney injury via enhancement of glomerular and tubular hypertrophy [96] and is associated with the progressive decline of glomerular filtration rates as a result of podocyte injury. Activation of the mTOR pathway is also implicated in the increased expression of profibrotic cytokines, such as TGF-β1 and connective tissue growth factor with subsequent interstitial fibrosis in diabetic nephropathy leading to the more glomerular lesion. Our results revealed that administration of EtOAc fraction improved the impaired autophagy induced by STZ. Previous investigations showed that increased phosphorylation of AMPK and decreased activation of its downstream, mTOR stimulated autophagy-related protection against DN [75]. The up-regulation of autophagic response by *P. peruviana* L EtOAc fraction was accompanied by decreased apoptosis. In consistence, previous studies showed that accelerated the accumulation of damaged mitochondria, resulting in apoptosis in response to impaired autophagy [97].

UPLC-ESI-MS/MS analysis was performed in positive and negative modes for the identification of the chemical composition of the bioactive EtOAc fraction. Eighteen phenolic compounds were identified in the EtOAc fraction based on comparing their high-resolution mass fragmentations with the reported literature. Chromatographic investigation of the bioactive EtOAc fraction led to the isolation of its 10 major compounds which were already detected in the UPLC-MS/MS analysis. Intriguingly, the in vitro antidiabetic activity performed on the isolated compounds revealed quercetin galactoside, quercetin rhamnoside, gallic acid, and methylellagic acid as promising candidates. Gallic acid was reported as amylase and glucosidase inhibitors [98,99]. In the current study, it showed a significant inhibition activity on both α-amylase and β-glucosidase enzymes. Quercetin-3-*O*-rhamnoside had a promising inhibitory effect on both α-amylase and β-glucosidase enzymes. Ellagic acid was also reported to have α-glucosidase inhibition activity [100], our results highlight the promising effect of its methyl derivative. Herein, we also reported the promising inhibitory activity of quercetin 3-*O*-galactoside on α-amylase and β-glucosidase enzymes. Our results are following previous reports that had shown that gallic acid, quercetin 3-*O*-α- rhamnoside, and ellagic acid have promising lipase inhibitory activity [101–103]. We herein report the lipase inhibitory activity of quercetin 3-*O*-galactoside and 3-*O*-methylellagic acid.

5. Conclusion

These results indicated that golden berry (*P. peruviana* L.) phenolics-rich fraction could prevent diabetic nephropathy by inhibiting apoptosis and stimulating autophagy via AMPK /mTOR signaling pathway. This suggests the involvement of autophagic up-regulation as a mechanism of the renoprotective effect of the golden berry against diabetic complications; particularly nephropathy. Moreover, our study is a step forward in drug discovery of natural products that can be used for the management of diabetes through α-amylase, lipase, and β-glucosidase inhibition activity. Furthermore, the quercetin glycosides, gallic acid as well as its methylated dimer represent promising candidates for screening antidiabetic metabolites from natural sources.

CRediT authorship contribution statement

Shahira M. Ezzat: Identification of the compounds, UPLC analysis-writing review & editing. **Heba M.I. Abdallah:** Writing – original draft & performing experimental Pharmacology. **Noha N. Yassen:** Histopathological study, Writing – original draft. **Rasha A. Radwan:** *In vitro* enzyme inhibition assays -Revising original draft. **Eman S. Mostafa:** Isolation of the compounds & their identification-revising the- original draft. **Maha M. Salama:** Writing – review & editing. **Mohamed A. Salem:** UPLC-ESI-MS/MS analysis & identification, Writing – original draft.

Conflict of interest statement

The authors have no conflict to declare.

Appendix A. Supporting information

Supplementary data associated with this article can be found in the online version at doi:10.1016/j.biopha.2021.111948.

References

[1] P. NS, The history of diabetes, in: G.T. Verlag (Ed.), The History of Diabetes Mellitus, Thieme, Stuttgart, 1964.
[2] H.P. Rang, M.M. Dale, J.M. Ritters, The Endocrine Pancreas and the Control of Blood Glucose; in Pharmacology, in: B. Simmons, S.U.K. Beasley (Eds.), Longman group Ltd, 1991, pp. 403–410.
[3] S. AK, Diabetes Mellitus and its Complications; An Update, in: E.O. Galadari, I. Behara, M. Manchandra, S.K. Adbulrazzaq, M.K. Mehra (Eds.), Macmillan, New Delhi, 1993.
[4] W. Xie, Y. Zhang, N. Wang, H. Zhou, L. Du, X. Ma, X. Shi, G. Cai, Novel effects of macrostemonoside A, a compound from Allium macrostemon Bung, on hyperglycemia, hyperlipidemia, and visceral obesity in high-fat diet-fed C57BL/6 mice, Eur. J. Pharmacol. 599 (1) (2008) 159–165.
[5] Y. Bains, A. Gugliucci, Ilex paraguariensis and its main component chlorogenic acid inhibit fructose formation of advanced glycation endproducts with amino acids at conditions compatible with those in the digestive system, Fitoterapia 117 (2017) 6–10.
[6] H. Gao, Y.-N. Huang, B. Gao, P. Li, C. Inagaki, J. Kawabata, Inhibitory effect on α-glucosidase by Adhatoda vasica Nees, Food Chem. 108 (3) (2008) 965–972.
[7] C.C. Cowie, F.K. Port, R.A. Wolfe, P.J. Savage, P.P. Moll, V.M. Hawthorne, Disparities in incidence of diabetic end-stage renal disease according to race and type of diabetes, New Engl. J. Med. 321 (16) (1989) 1074–1079.
[8] M. Aurell, S. BjöRck, Determinants of progressive renal disease in diabetes mellitus, Kidney Int. Suppl. 36 (1992) 38–42.
[9] C. Tomás-Zapico, A. Coto-Montes, Melatonin as antioxidant under pathological processes, Recent Patents Endocr. Metab. Immune Drug Discov. 1 (1) (2007) 63–82.
[10] H. Abe, T. Matsubara, H. Arai, Role of Smad1 in diabetic nephropathy: molecular mechanisms and implications as a diagnostic marker, Histol. Histopathol. Vol. 26 (no 4) (2011) (2011).
[11] P. Jiang, N. Mizushima, Autophagy and human diseases, Cell Res. 24 (1) (2014) 69–79.
[12] F.M. Menzies, A. Fleming, D.C. Rubinsztein, Compromised autophagy and neurodegenerative diseases, Nat. Rev. Neurosci. 16 (6) (2015) 345–357.
[13] K. Inoue, H. Kuwana, Y. Shimamura, K. Ogata, Y. Taniguchi, T. Kagawa, T. Horino, T. Takao, T. Morita, S. Sasaki, Cisplatin-induced macroautophagy occurs prior to apoptosis in proximal tubules in vivo, Clin. Exp. Nephrol. 14 (2) (2010) 112–122.

[14] S. Kume, T. Uzu, K. Horiike, M. Chin-Kanasaki, K. Isshiki, S.-i Araki, T. Sugimoto, M. Haneda, A. Kashiwagi, D. Koya, Calorie restriction enhances cell adaptation to hypoxia through Sirt1-dependent mitochondrial autophagy in mouse aged kidney, J. Clin. Investig. 120 (4) (2010) 1043–1055.

[15] T. Kimura, Y. Takabatake, A. Takahashi, J.-y Kaimori, I. Matsui, T. Namba, H. Kitamura, F. Niimura, T. Matsusaka, T. Soga, Autophagy protects the proximal tubule from degeneration and acute ischemic injury, J. Am. Soc. Nephrol. 22 (5) (2011) 902–913.

[16] Y. Tanaka, S. Kume, M. Kitada, K. Kanasaki, T. Uzu, H. Maegawa, D. Koya, Autophagy as a therapeutic target in diabetic nephropathy, Exp. Diabetes Res. (2012 () (2011).

[17] H.A. Chatzigeorgiou A, K. Kalafatakis, E. Kamper, The use of animal models in the study of diabetes mellitus, Vivo 23 (2009) 245–258.

[18] E.K. Eleazu CO, S. Chukwuma, U.N. Essien, Review of the mechanism of cell death resulting from streptozotocin challenge in experimental animals, its practical use and potential risk to humans, J. Diabetes Metab. Disord. 12 (1) (2013) 60–67.

[19] A.J. Rees DA, Animal models of diabetes mellitus, Diabet. Med. 22 (2005) 359–370.

[20] S. T, The mechanism of alloxan and streptozotocin action in B cells of the rat pancreas, Physiol. Res. Acad. Sci. Bohemoslov. 50 (2001) 537–546.

[21] M. Hahn, P.P. van Krieken, C. Nord, T. Alanentalo, F. Morini, Y. Xiong, M. Eriksson, J. Mayer, E. Kostromina, J.L. Ruas, Topologically selective islet vulnerability and self-sustained downregulation of markers for β-cell maturity in streptozotocin-induced diabetes, Commun. Biol. 3 (1) (2020) 1–14.

[22] G.H. Wang Z, GLUT2 in pancreatic islets: crucial target molecule in diabetes induced with multiple low doses of streptozotocin in mice, Diabetes 47 (1998) 50–56.

[23] K.T. Imaeda A, T. Aoki, Y. Kondo, H. Nagase, DNA damage and the effect of antioxidants in streptozotocin-treated mice, Food Chem. Toxicol. 40 (2002) 979–987.

[24] W.Y. Tay YC, L. Kairaitis, G.K. Rangan, C. Zhang, D.C. Harris, Can murine diabetic nephropathy be separated from superimposed acute renal failure? Kidney Int 68 (2005) 391–398.

[25] C.J. Bailey, C. Day, Traditional plant medicines as treatments for diabetes, Diabetes Care 12 (8) (1989) 553–564.

[26] K. Shapiro, W.C. Gong, Natural products used for diabetes, J. Am. Pharm. Assoc. 42 (2) (2002) 217–226.

[27] D. Klinac, Cape gooseberry (*Physalis peruviana*) production systems, N.Z. J. Exp. Agric. 14 (4) (1986) 425–430.

[28] Y.-H. Lan, F.-R. Chang, M.-J. Pan, C.-C. Wu, S.-J. Wu, S.-L. Chen, S.-S. Wang, M.-J. Wu, Y.-C. Wu, New cytotoxic withanolides from *Physalis peruviana*, Food Chem. 116 (2) (2009) 462–469.

[29] H. Mayorga, C. Duque, H. Knapp, P. Winterhalter, Hydroxyester disaccharides from fruits of cape gooseberry (Physalis peruviana), Phytochemistry 59 (4) (2002) 439–445.

[30] B. Dong, L. An, X. Yang, X. Zhang, J. Zhang, M. Tuerhong, D.-Q. Jin, Y. Ohizumi, D. Lee, J. Xu, Withanolides from *Physalis peruviana* showing nitric oxide inhibitory effects and affinities with iNOS, Bioorg. Chem. 87 (2019) 585–593.

[31] S.M. Llano, A.M. Muñoz-Jiménez, C. Jiménez-Cartagena, J. Londoño-Londoño, S. Medina, Untargeted metabolomics reveals specific withanolides and fatty acyl glycoside as tentative metabolites to differentiate organic and conventional *Physalis peruviana* fruits, Food Chem. 244 (2018) 120–127.

[32] M.F. Ramadan, Bioactive phytochemicals, nutritional value, and functional properties of cape gooseberry (*Physalis peruviana*): an overview, Food Res. Int. 44 (7) (2011) 1830–1836.

[33] M.-L. Olivares-Tenorio, M. Dekker, R. Verkerk, M.A. van Boekel, Health-promoting compounds in cape gooseberry (*Physalis peruviana* L.): review from a supply chain perspective, Trends Food Sci. Technol. 57 (2016) 83–92.

[34] S.-J. Wu, L.-T. Ng, D.-L. Lin, S.-N. Huang, S.-S. Wang, C.-C. Lin, *Physalis peruviana* extract induces apoptosis in human Hep G2 cells through CD95/CD95L system and the mitochondrial signaling transduction pathway, Cancer Lett. 215 (2) (2004) 199–208.

[35] H.F. El-Mehiry, H. Helmy, M.A. El-Ghany, Antidiabetic and antioxidative activity of physalis powder or extract with chromium in rats, World J. Med. Sci. 7 (2012) 27–33.

[36] M. Sathyadevi, E. Suchithra, S. Subramanian, *Physalis peruviana* Linn. fruit extract improves insulin sensitivity and ameliorates hyperglycemia in high-fat diet low dose STZ-induced type 2 diabetic rats, J. Pharm. Res. 8 (4) (2014) 625–632.

[37] S. Poovitha, M. Parani, In vitro and in vivo α-amylase and α-glucosidase inhibiting activities of the protein extracts from two varieties of bitter gourd (Momordica charantia L.), BMC Complement. Altern. Med. 16 Suppl 1 (1) (2016) 185.

[38] L.M. Salazinik, S. ve Usnik, Glucosidase Inhibitory and Radical Scavenging Properties of Lichen Metabolites Salazinic Acid, Sekikaic Acid and Usnic Acid.

[39] F. Conforti, V. Perri, F. Menichini, M. Marrelli, D. Uzunov, G.A. Statti, F. Menichini, Wild Mediterranean dietary plants as inhibitors of pancreatic lipase, Phytother. Res. 26 (2012) 600–604.

[40] K. Mishra, H. Ojha, N.K. Chaudhury, Estimation of antiradical properties of antioxidants using DPPH assay: a critical review and results, Food Chem. 130 (4) (2012) 1036–1043.

[41] W. Brand-Williams, M.E. Cuvelier, C. Berset, Use of a free radical method to evaluate antioxidant activity, LWT Food Sci. Technol. 28 (1) (1995) 25–30.

[42] C. Lucas-Abellan, M.T. Mercader-Ros, M.P. Zafrilla, M.I. Fortea, J.A. Gabaldon, E. Nunez-Delicado, ORAC-fluorescein assay to determine the oxygen radical absorbance capacity of resveratrol complexed in cyclodextrins, J. Agric. Food Chem. 56 (6) (2008) 2254–2259.

[43] N.M. Hegazi, R.A. Radwan, S.M. Bakry, H.H. Saad, Molecular networking aided metabolomic profiling of beet leaves using three extraction solvents and in relation to its anti-obesity effects, J. Adv. Res. 24 (2020) 545–555.

[44] S.M. Ezzat, A. Abdel Motaal, S.A.W. El Awdan, In vitro and in vivo antidiabetic potential of extracts and a furostanol saponin from Balanites aegyptiaca, Pharm. Biol. 55 (1) (2017) 1931–1936.

[45] G. Brosky, J. Logothetopoulos, Streptozotocin diabetes in the mouse and guinea pig, Diabetes 18 (9) (1969) 606–611.

[46] M.A. Salem, T. Yoshida, L. Perez de Souza, S. Alseekh, K. Bajdzienko, A.R. Fernie, P. Giavalisco, An improved extraction method enables the comprehensive analysis of lipids, proteins, metabolites and phytohormones from a single sample of leaf tissue under water-deficit stress, Plant J. 103 (2020) 1614–1632.

[47] S.A.Ld Moura, G. Negri, A. Salatino, L.Dd.C. Lima, L.P.A. Dourado, J.B. Mendes, S.P. Andrade, M.A.N.D. Ferreira, D.C. Cara, Aqueous extract of Brazilian green propolis: primary components, evaluation of inflammation and wound healing by using subcutaneous implanted sponges, Evid. -Based Complement. Altern. Med. 2011 (2011)) (2011) 1–8.

[48] J.D. Djoukeng, V. Arbona, R. Argamasilla, A. Gomez-Cadenas, Flavonoid profiling in leaves of citrus genotypes under different environmental situations, J. Agric. Food Chem. 56 (23) (2008) 11087–11097.

[49] M.E. Karar, N. Kuhnert, UPLC-ESI-Q-TOF-MS/MS characterization of phenolics from Crataegus monogyna and Crataegus laevigata (Hawthorn) leaves, fruits and their herbal derived drops (Crataegutt Tropfen), J. Chem. Biol. Ther. 1 (102) (2015) 2572–0406.1000102.

[50] K. Aaby, D. Ekeberg, G. Skrede, Characterization of phenolic compounds in strawberry (Fragaria× ananassa) fruits by different HPLC detectors and contribution of individual compounds to total antioxidant capacity, J. Agric. Food Chem. 55 (11) (2007) 4395–4406.

[51] L.-Z. Lin, J.M. Harnly, Identification of the phenolic components of collard greens, kale, and Chinese broccoli, J. Agric. Food Chem. 57 (16) (2009) 7401–7408.

[52] T. Hofmann, E. Nebehaj, L. Albert, Antioxidant properties and detailed polyphenol profiling of European hornbeam (Carpinus betulus L.) leaves by multiple antioxidant capacity assays and high-performance liquid chromatography/multistage electrospray mass spectrometry, Ind. Crops Prod. 87 (2016) 340–349.

[53] S. Sang, C.S. Yang, Structural identification of novel glucoside and glucuronide metabolites of (−)-epigallocatechin-3–gallate in mouse urine using liquid chromatography/electrospray ionization tandem mass spectrometry, Rapid Commun. Mass Spectrom. 22 (22) (2008) 3693–3699.

[54] M. Nawwar, N. Swilam, A. Hashim, A. Al-Abd, A. Abdel-Naim, U. Lindequist, Cytotoxic isoferulic acidamide from Myricaria germanica (Tamaricaceae), Plant Signal. Behav. 8 (1) (2013) 22642.

[55] H.-H. Lee, J.-Y. Cho, J.-H. Moon, K.-H. Park, Isolation and identification of antioxidative phenolic acids and flavonoid glycosides from Camellia japonica flowers, Hortic. Environ. Biotechnol. 52 (3) (2011) 270–277.

[56] C. Pereira, C.B. Barreto Júnior, R.M. Kuster, N.K. Simas, C.M. Sakuragui, A. Porzel, L. Wessjohann, Flavonoids and a neolignan glucoside from Guarea macrophylla (Meliaceae), Quím. Nova 35 (6) (2012) 1123–1126.

[57] S. Othman, M. El-Hashash, S. Hussein, A. El-Mesallamy, S. Rizk, F.A. Elabbar, Phenolic content as antioxidant and antimicrobial activities of pistacia atlantica desf.(anacardiaceae) extract from libya, Egypt. J. Chem. 62 (1) (2019) 21–28.

[58] M. Nawwar, N. Youb, M. El-Raey, S. Zaghloul, A. Hashem, E. Mostafa, O. Eldahshan, V. Werner, A. Becker, B. Haertel, Polyphenols in Ammania auriculata: structures, antioxidative activity and cytotoxicity, Die Pharm. Int. J. Pharm. Sci. 69 (11) (2014) 860–864.

[59] J. Chen, J. Teng, L. Ma, H. Tong, B. Ren, L. Wang, W. Li, Flavonoids isolated from the flowers of Limonium bicolor and their in vitro antitumor evaluation, Pharmacogn. Mag. 13 (50) (2017) 222–225.

[60] P.K. Jain, A. Patra, S. Satpathy, S. Jain, S. Khan, Antibacterial and antioxidant activities of 3-O-methyl ellagic acid from stem bark of polyalthia longifolia thw, Chiang Mai J. Sci. 45 (2) (2018) 858–867.

[61] A.-N. Kawde, M. Taha, R.S. Alansari, N.B. Almandil, N. Uddin, F. Rahim, S. Chigurupati, M. Nawaz, S. Hayat, M. Ibrahim, Exploring efficacy of indole-based dual inhibitors for α-glucosidase and α-amylase enzymes: in silico, biochemical and kinetic studies, Int. J. Biol. Macromol. 154 (2020) 217–232.

[62] U. Salar, K.M. Khan, S. Chigurupati, M. Taha, A. Wadood, S. Vijayabalan, M. Ghufran, S. Perveen, New hybrid hydrazinyl thiazole substituted chromones: as potential α-amylase inhibitors and radical (DPPH & ABTS) scavengers, Sci. Rep. 7 (1) (2017) 1–17.

[63] H. Sun, D. Wang, X. Song, Y. Zhang, W. Ding, X. Peng, X. Zhang, Y. Li, Y. Ma, R. Wang, Natural prenylchalconaringenins and prenylnaringenins as antidiabetic agents: α-glucosidase and α-amylase inhibition and in vivo antihyperglycemic and antihyperlipidemic effects, J. Agric. Food Chem. 65 (8) (2017) 1574–1581.

[64] C. Rask-Madsen, G.L. King, Vascular complications of diabetes: mechanisms of injury and protective factors, Cell Metab. 17 (1) (2013) 20–33.

[65] L. Katznelson, E.R. Laws Jr., S. Melmed, M.E. Molitch, M.H. Murad, A. Utz, J. A. Wass, Acromegaly: an endocrine society clinical practice guideline, J. Clin. Endocrinol. Metab. 99 (11) (2014) 3933–3951.

[66] J. Wu, L.-J. Yan, Streptozotocin-induced type 1 diabetes in rodents as a model for studying mitochondrial mechanisms of diabetic β cell glucotoxicity, Diabetes Metab. Syndr. Obes. 8 (2015) 181–188.

[67] S. Lenzen, The mechanisms of alloxan-and streptozotocin-induced diabetes, Diabetologia 51 (2) (2008) 216–226.

[68] M. Zafar, Adverse events among the elderly receiving chemotherapy for advanced non-small-cell lung cancer, J. Clin. Oncol. Off. J. Am. Soc. Clin. Oncol. 28 (1) (2010) 620–627.
[69] F. Howarth, M. Jacobson, M. Shafiullah, E. Adeghate, Long-term effects of streptozotocin-induced diabetes on the electrocardiogram, physical activity and body temperature in rats, Exp. Physiol. 90 (6) (2005) 827–835.
[70] D. Campbell, R. Lavielle, C. Nathan, The mode of action and clinical pharmacology of gliclazide: a review, Diabetes Res. Clin. Pract. 14 (1991) S21–S36.
[71] B.L. Wajchenberg, A.T.M. Santomauro, R.N. Porrelli, Effect of a sulfonylurea (gliclazide) treatment on insulin sensitivity and glucose-mediated glucose disposal in patients with non-insulin-dependent diabetes mellitus (NIDDM), Diabetes Res. Clin. Pract. 20 (2) (1993) 147–154.
[72] M.K. Arora, U.K. Singh, Molecular mechanisms in the pathogenesis of diabetic nephropathy: an update, Vasc. Pharmacol. 58 (4) (2013) 259–271.
[73] S. Shrestha, P. Gyawali, R. Shrestha, B. Poudel, M. Sigdel, Serum urea and creatinine in diabetic and non-diabetic subjects, J. Nepal Assoc. Med. Lab. Sci. P 11 (2008) 12.
[74] M. Anjaneyulu, K. Chopra, Quercetin, an anti-oxidant bioflavonoid, attenuates diabetic nephropathy in rats, Clin. Exp. Pharmacol. Physiol. 31 (4) (2004) 244–248.
[75] J. Zhang, R. Zhang, Y. Wang, H. Li, Q. Han, Y. Wu, T. Wang, F. Liu, The level of serum albumin is associated with renal prognosis in patients with diabetic nephropathy, J. Diabetes Res. 2019 (2019 () (2019) 1–9.
[76] L.A. Ahmed, Renoprotective effect of Egyptian cape gooseberry fruit (*Physalis peruviana* L.) against acute renal injury in rats, Sci. World J. (2014 () (2014).
[77] S.E. El-Gengaihi, M.A. Hamed, A.E.-R.M. Khalaf-Allah, M.A. Mohammed, Golden berry juice attenuates the severity of hepatorenal injury, J. Diet. Suppl. 10 (4) (2013) 357–369.
[78] D. Nocetti, C. Sacristán, P. Ruiz, J. Guerrero, G. Jorquera, E. Uribe, J.L. Bucarey, A. Espinosa, L. Puente, *Physalis peruviana* L. pulp prevents liver inflammation and insulin resistance in skeletal muscles of diet-induced obese mice, Nutrients 12 (3) (2020) 700.
[79] C. Srimaroeng, A. Ontawong, N. Saowakon, P. Vivithanaporn, A. Pongchaidecha, D. Amornlerdpison, S. Soodvilai, V. Chatsudthipong, Antidiabetic and renoprotective effects of Cladophora glomerata Kützing extract in experimental type 2 diabetic rats: a potential nutraceutical product for diabetic nephropathy, J. Diabetes Res. (2015 () (2015).
[80] B.R. Latti, S.B. Birajdar, R.G. Latti, Periodic acid schiff-diastase as a key in exfoliative cytology in diabetics: a pilot study, J. Oral. Maxillofac. Pathol.: JOMFP 19 (2) (2015) 188–191.
[81] M. Torbenson, Y.-Y. Chen, E. Brunt, O.W. Cummings, M. Gottfried, S. Jakate, Y.-C. Liu, M.M. Yeh, L. Ferrell, Glycogenic hepatopathy: an underrecognized hepatic complication of diabetes mellitus, Am. J. Surg. Pathol. 30 (4) (2006) 508–513.
[82] S. Tanaka, K. Aida, Y. Nishida, T. Kobayashi, Pathophysiological mechanisms involving aggressive islet cell destruction in fulminant type 1 diabetes, Endocr. J. 60 (2013) 837–845.
[83] J. Meier, A. Bhushan, A. Butler, R. Rizza, P. Butler, Sustained beta cell apoptosis in patients with long-standing type 1 diabetes: indirect evidence for islet regeneration? Diabetologia 48 (11) (2005) 2221–2228.
[84] G. Orlando, P. Gianello, M. Salvatori, R.J. Stratta, S. Soker, C. Ricordi, J. Domínguez-Bendala, Cell replacement strategies aimed at reconstitution of the β-cell compartment in type 1 diabetes, Diabetes 63 (5) (2014) 1433–1444.
[85] K. Turkmen, Inflammation, oxidative stress, apoptosis, and autophagy in diabetes mellitus and diabetic kidney disease: the Four horsemen of the apocalypse, Int. Urol. Nephrol. 49 (5) (2017) 837–844.
[86] Q. Lu, Y. Zhou, M. Hao, C. Li, J. Wang, F. Shu, L. Du, X. Zhu, Q. Zhang, X. Yin, The mTOR promotes oxidative stress-induced apoptosis of mesangial cells in diabetic nephropathy, Mol. Cell. Endocrinol. 473 (2018) 31–43.
[87] H.A. Hassan, H.M. Serag, M.S. Qadir, M.F.R. Hassanien, Cape gooseberry (*Physalis peruviana*) juice as a modulator agent for hepatocellular carcinoma-linked apoptosis and cell cycle arrest, Biomed. Pharmacother. 94 (2017) 1129–1137.
[88] M.A. Dkhil, S. Al-Quraishy, M.M. Diab, M.S. Othman, A.M. Aref, A.E.A. Moneim, The potential protective role of *Physalis peruviana* L. fruit in cadmium-induced hepatotoxicity and nephrotoxicity, Food Chem. Toxicol. 74 (2014) 98–106.
[89] S.N. Uwaezuoke, The role of novel biomarkers in predicting diabetic nephropathy: a review, Int. J. Nephrol. Renov. Dis. 10 (2017) 221–231.
[90] A. Tagawa, M. Yasuda, S. Kume, K. Yamahara, J. Nakazawa, M. Chin-Kanasaki, H. Araki, S.-i Araki, D. Koya, K. Asanuma, Impaired podocyte autophagy exacerbates proteinuria in diabetic nephropathy, Diabetes 65 (3) (2016) 755–767.
[91] I. Tanida, N. Minematsu-Ikeguchi, T. Ueno, E. Kominami, Lysosomal turnover, but not a cellular level, of endogenous LC3 is a marker for autophagy, Autophagy 1 (2) (2005) 84–91.
[92] R. Li, P. Zhou, Y. Guo, J.-S. Lee, B. Zhou, Tris (1, 3-dichloro-2-propyl) phosphate induces apoptosis and autophagy in SH-SY5Y cells: Involvement of ROS-mediated AMPK/mTOR/ULK1 pathways, Food Chem. Toxicol. 100 (2017) 183–196.
[93] D.-F. Ding, N. You, X.-M. Wu, J.-R. Xu, A.-P. Hu, X.-L. Ye, Q. Zhu, X.-Q. Jiang, H. Miao, C. Liu, Resveratrol attenuates renal hypertrophy in early-stage diabetes by activating AMPK, Am. J. Nephrol. 31 (4) (2010) 363–374.
[94] J. Kim, M. Kundu, B. Viollet, K.-L. Guan, AMPK and mTOR regulate autophagy through direct phosphorylation of Ulk1, Nat. Cell Biol. 13 (2) (2011) 132–141.
[95] S. Alers, A.S. Löffler, S. Wesselborg, B. Stork, Role of AMPK-mTOR-Ulk1/2 in the regulation of autophagy: cross talk, shortcuts, and feedbacks, Mol. Cell. Biol. 32 (1) (2012) 2–11.
[96] M. Gödel, B. Hartleben, N. Herbach, S. Liu, S. Zschiedrich, S. Lu, A. Debreczeni-Mór, M.T. Lindenmeyer, M.-P. Rastaldi, G. Hartleben, Role of mTOR in podocyte function and diabetic nephropathy in humans and mice, J. Clin. Investig. 121 (6) (2011) 2197–2209.
[97] X.-X. Zhang, C.-H. Jiang, Y. Liu, D.-X. Lou, Y.-P. Huang, M. Gao, J. Zhang, Z.-Q. Yin, K. Pan, Cyclocarya paliurus triterpenic acids fraction attenuates kidney injury via AMPK-mTOR-regulated autophagy pathway in diabetic rats, Phytomedicine 64 (2019), 153060.
[98] S.A. Adefegha, G. Oboh, I.I. Ejakpovi, S.I. Oyeleye, Antioxidant and antidiabetic effects of gallic and protocatechuic acids: a structure–function perspective, Comp. Clin. Pathol. 24 (6) (2015) 1579–1585.
[99] G. Oboh, O.B. Ogunsuyi, M.D. Ogunbadejo, S.A. Adefegha, Influence of gallic acid on α-amylase and α-glucosidase inhibitory properties of acarbose, J. Food Drug Anal. 24 (3) (2016) 627–634.
[100] Q. You, F. Chen, X. Wang, Y. Jiang, S. Lin, Anti-diabetic activities of phenolic compounds in muscadine against alpha-glucosidase and pancreatic lipase, LWT-Food Sci. Technol. 46 (1) (2012) 164–168.
[101] P.V. Dludla, B.B. Nkambule, B. Jack, Z. Mkandla, T. Mutize, S. Silvestri, P. Orlando, L. Tiano, J. Louw, S.E. Mazibuko-Mbeje, Inflammation and oxidative stress in an obese state and the protective effects of gallic acid, Nutrients 11 (1) (2019) 23.
[102] C. Zhang, Y. Ma, Y. Zhao, Y. Hong, S. Cai, M. Pang, Phenolic composition, antioxidant and pancreatic lipase inhibitory activities of Chinese sumac (Rhus chinensis Mill.) fruits extracted by different solvents and interaction between myricetin-3–O-rhamnoside and quercetin-3–O-rhamnoside, Int. J. Food Sci. Technol. 53 (4) (2018) 1045–1053.
[103] B. Saad, H. Zaid, S. Shanak, S. Kadan, Herbal-derived anti-obesity compounds and their action mechanisms. Anti-diabetes and Anti-obesity Medicinal Plants and Phytochemicals, Springer, 2017, pp. 129–144.